

the scalar product between two eigendifferentials  $\bar{\psi}_1$  and  $\bar{\psi}_2$ , centered at  $\mathbf{x}$  and  $\mathbf{y}$ , respectively, is

$$(\bar{\psi}_1, \bar{\psi}_2) = (2\pi)^{-3} m^2 \times \int_{S(\epsilon, \mathbf{x})} d^3x' \int_{S(\epsilon, \mathbf{y})} d^3y' \frac{K_1(m|\mathbf{x}' - \mathbf{y}'|)}{m|\mathbf{x}' - \mathbf{y}'|}. \quad (20)$$

Since the Bessel function  $K_1(z)$  is always positive for  $z > 0$ , this scalar product is positive and nonzero for

arbitrarily large distances  $|\mathbf{x} - \mathbf{y}|$  between the spheres in which the eigendifferentials are formed. Thus Lorentz-invariant localization, as we have formulated it, does not lead to orthogonal localized states.

The nonorthogonality of the eigendifferentials means that there is no self-adjoint operator ("position operator") which has the localized state (17) in its continuous spectrum. This constitutes an unfortunate consequence of the decision to drop the orthogonality requirement included in the NW postulates.

## Many-Body Perturbation Theory Applied to Atoms\*

HUGH P. KELLY

*Department of Physics, University of California, San Diego, La Jolla, California*

(Received 29 June 1964)

Many-body perturbation theory as formulated by Brueckner and Goldstone is applied to atoms to obtain corrections to Hartree-Fock wave functions and energies. Calculations are made using a complete set of single-particle Hartree-Fock wave functions which includes both the continuum and an infinite number of bound states. It is shown how one may readily perform the sums over an infinite number of bound excited states. In order to demonstrate the usefulness of many-body perturbation theory in atomic problems, calculations are made for a wide variety of properties of the neutral beryllium atom. The calculated  $2s$ - $2s$  correlation energy is  $-0.0436$  atomic unit for  $l=1$  excitations. The calculated dipole and quadrupole polarizabilities are  $6.93 \times 10^{-24}$  cm<sup>3</sup> and  $14.1 \times 10^{-40}$  cm<sup>5</sup>, respectively. The calculated dipole and quadrupole shielding factors are 0.972 and 0.75. Results are given for oscillator strengths, photoionization cross sections, and the Thomas-Reiche-Kuhn sum rule, which is 4.14 as compared with 4.00, the theoretical value.

### I. INTRODUCTION

MANY-BODY perturbation theory as developed by Brueckner<sup>1</sup> and Goldstone<sup>2</sup> has proven very useful in the study of many-particle systems. As shown by Brueckner, the appropriate form of perturbation theory as the number of particles becomes large is Rayleigh-Schrödinger theory modified so as to eliminate the "unlinked clusters." The principal applications of the Brueckner-Goldstone linked cluster expansion (BG expansion) to many-fermion systems have thus far been investigations of nuclear structure<sup>3</sup> and of the electron gas.<sup>4</sup> However, the BG theory, which corrects both wave functions and energies, should also prove very useful in calculations of atomic structure and in other fields. In applying this theory to atoms, where the interparticle forces are well known, one also gains information as to its general applicability to finite systems.

A previous application of BG theory to the calculation of correlation energies in the neutral beryllium atom yielded excellent results.<sup>5</sup> However, it was found necessary to calculate high orders in the expansion. This difficulty was related to the set of single-particle Hartree-Fock states which were used. The purpose of this paper is to investigate the use of a different basis set for the expansion and to show the usefulness of perturbation calculations using this set. The states used are the ground-state Hartree-Fock orbitals and single-particle excitations calculated in the Hartree-Fock potential field of the nucleus and  $N-1$  of the  $N$  ground-state orbitals. The use of this set is justified in Sec. II. In Sec. III it is shown how sums over an infinite number of bound excited states may be carried out. In Sec. IV the  $l=1$  correlation energy among the two  $2s$  electrons of Be is calculated. In Sec. V calculations are given for the dipole and quadrupole polarizabilities and shielding factors for Be. In Sec. VI many oscillator strengths and the photoionization cross section curve are calculated. Section VII contains the conclusions.

\* Work supported in part by the U. S. Atomic Energy Commission.

<sup>1</sup> K. A. Brueckner, Phys. Rev. **97**, 1353 (1955); **100**, 36 (1955); *The Many-Body Problem* (John Wiley & Sons, Inc., New York, 1959).

<sup>2</sup> J. Goldstone, Proc. Roy. Soc. (London) **A239**, 267 (1957).

<sup>3</sup> K. A. Brueckner and J. L. Gammel, Phys. Rev. **109**, 1023 (1958); K. A. Brueckner and K. S. Masterson, Jr., *ibid.* **128**, 2267 (1962).

<sup>4</sup> M. Gell-Mann and K. Brueckner, Phys. Rev. **106**, 364 (1957).

<sup>5</sup> H. P. Kelly, Phys. Rev. **131**, 684 (1963), hereafter referred to as K. Correlation energies are defined in K.

II. PERTURBATION THEORY

A. Review of the Brueckner-Goldstone Expansion

The total Hamiltonian for a system of  $N$  identical fermions interacting through two-body potentials  $v_{ij}$  is

$$H = \sum_{i=1}^N T_i + \sum_{i<j}^N v_{ij}. \tag{1}$$

The kinetic energy for the  $i$ th particle and the sum of all one-body potentials acting on it are given by  $T_i$ . For atoms  $T_i$  includes the interaction of the  $i$ th electron with the nucleus. The true ground state of the system is  $\Psi_0$  given by

$$H\Psi_0 = (E_0 + \Delta E)\Psi_0. \tag{2}$$

The effect of the  $N$  interacting particles may be approximated by a single-particle potential  $V$  and then  $\Psi_0$  is approximated by  $\Phi_0$  where

$$H_0\Phi_0 = E_0\Phi_0 \tag{3}$$

and

$$H_0 = \sum_{i=1}^N (T_i + V_i). \tag{4}$$

The single-particle wave functions,  $\varphi_n$  which are solutions of

$$(T + V)\varphi_n = \epsilon_n\varphi_n, \tag{5}$$

constitute an orthonormal set, provided  $V$  is Hermitian. The state  $\Phi_0$  is a determinant formed from the  $N$  solutions of Eq. (5) which are lowest in energy. The states occupied in  $\Phi_0$  are called unexcited states. An unoccupied unexcited state is called a hole and an occupied excited state is called a particle.

The BG result is that

$$\Psi_0 = \sum_L \left( \frac{1}{E_0 - H_0} H' \right)^n \Phi_0, \tag{6}$$

where  $\sum_L$  means that only "linked" terms are to be included<sup>2</sup> and

$$H' = \sum_{i<j}^N v_{ij} - \sum_{i=1}^N V_i. \tag{7}$$

Also,

$$\Delta E = \sum_{L'} \langle \Phi_0 | H' \left( \frac{1}{E_0 - H_0} H' \right)^n | \Phi_0 \rangle, \tag{8}$$

where  $L'$  indicates that the sum is only over those terms which are "linked" when the leftmost  $H'$  interaction is removed.

To first order, the energy is

$$E^{(1)} = E_0 + \langle \Phi_0 | H' | \Phi_0 \rangle, \tag{9}$$

and when a Hartree-Fock basis is used

$$E^{(1)} = E_{\text{HF}} + \sum_{n=1}^N (\langle n | T | n \rangle + \frac{1}{2} \langle n | V | n \rangle). \tag{10}$$

B. Choice of the Single-Particle Potential  $V$

The Hartree-Fock potential is defined by<sup>2</sup>

$$\langle a | V_{\text{HF}} | b \rangle = \sum_{n=1}^N (\langle an | v | bn \rangle - \langle an | v | nb \rangle), \tag{11}$$

where  $a$  and  $b$  are arbitrary. This potential was used in  $K$  to obtain the complete set of single-particle Hartree-Fock states which were used in calculating the correlation energy for Be. When  $V_{\text{HF}}$  is used, Eq. (5) for the single-particle states  $\varphi_n$  becomes

$$-\frac{1}{2}\nabla^2\varphi_n(\mathbf{r}) - Z/r\varphi_n(\mathbf{r}) + \left( \sum_{j=1}^N \int d\mathbf{r}' \frac{\varphi_j^*(\mathbf{r}')\varphi_j(\mathbf{r}')}{|\mathbf{r}-\mathbf{r}'|} \right) \varphi_n(\mathbf{r}) - \sum_{j=1}^N \left( \delta(m_{sn}, m_{sj}) \int d\mathbf{r}' \frac{\varphi_j^*(\mathbf{r}')\varphi_n(\mathbf{r}')}{|\mathbf{r}-\mathbf{r}'|} \varphi_j(\mathbf{r}) \right) = \epsilon_n\varphi_n(\mathbf{r}). \tag{12}$$

This is the usual Hartree-Fock equation considered, for example, by Slater.<sup>6</sup> Atomic units are used throughout this paper except where specified otherwise. Once the  $N$  unexcited states have been calculated self-consistently by solving the coupled Eqs. (12),  $V_{\text{HF}}$  is determined and the remaining states of the orthonormal set are obtained by solving the single Eq. (12). As pointed out in  $K$ , excited states are calculated in the potential of  $N$  particles but unexcited states are calculated in the potential of  $N-1$  particles because of cancellation of direct and exchange terms when  $\varphi_j = \varphi_n$ . In  $K$  this led to the surprising result that all excited single-particle Hartree-Fock states for Be were in the continuum and it was conjectured that excited states of Eq. (12) would all lie in the continuum for most if not all neutral atoms.

There are two advantages in dealing with only continuum excited states. First, it is much simpler to solve Eq. (12) for continuum states than for bound states for which it becomes an eigenvalue equation. Second, sums over excited states are more readily performed when only continuum excited states need be considered. However, in the numerical work reported in the later sections of this paper it was found quite feasible both to solve Eq. (12) for bound states and to sum over excited bound and continuum states. There is also a disadvantage in using  $V_{\text{HF}}$  as defined by Eqs. (11) or (12) for excited states. In  $K$  it was found that the perturbation expansion converged slowly for the correlation energy among  $2s$  electrons; this was due to large effects from certain hole-particle interactions referred to as second-type EPV (exclusion-principle-violating) diagrams. They were shown to arise from the fact that interactions of excited particles with the occupied unexcited states do not cancel the interaction with  $V_{\text{HF}}$  as shown in Fig. 1.

<sup>6</sup> J. C. Slater, *Quantum Theory of Atomic Structure* (McGraw-Hill Book Company, Inc., New York, 1960), Vol. II, Chap. 17, p. 6.

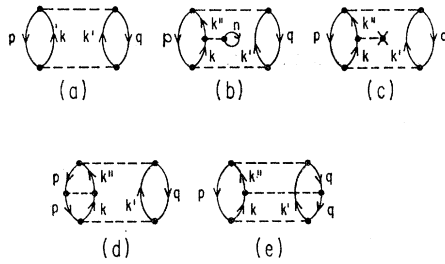


FIG. 1. (a) Second-order energy diagram. (b) Particle in excited state  $\varphi_k$  interacts with all occupied unexcited states  $\varphi_n$ . Note that  $\varphi_p$  and  $\varphi_q$  are no longer occupied. (c) Particle in state  $\varphi_k$  interacts with the potential  $V$ . When the Hartree-Fock potential  $V_{HF}$  of Eq. (11) is used, diagram (b) does not fully cancel (c) because  $V_{HF}$  includes interactions with all unexcited states. Diagrams (d) and its exchange and (e) result. If  $\varphi_p$  and  $\varphi_q$  have parallel spins there is also the exchange of diagram (e). There are similar diagrams for the interactions of  $\varphi_{k'}$ .

Since the excited particles actually interact with  $N-1$  other particles, it appears desirable to choose the potential accordingly.<sup>7</sup> In the calculations of this paper for Be the excited states were calculated in the potential field of the nucleus and  $(1s)^2(2s)$  where  $1s$  and  $2s$  are the Hartree-Fock orbitals of the neutral beryllium atom. In this potential the excited states have direct interactions with two  $1s$  electrons and one  $2s$  electron and also an exchange interaction with one  $1s$  electron. The excited states then correspond closely to the physical single-particle excitations of beryllium. The  $2s$  state for this potential coincides with the usual Hartree-Fock  $2s$  state. The new  $1s$  state differs from the Hartree-Fock solution but this difference is expected to be small as the  $1s$  potential depends strongly on the interaction with the nucleus. However, there are now first-order corrections to the wave function as shown in Fig. 2. When these terms and similar terms in higher orders are added to  $\Phi_0$  the wave function becomes the usual Hartree-Fock  $\Phi_0$ . The appropriate procedure is to omit

TABLE I. Orthogonality of  $s$  states.<sup>a</sup>

$\langle 1s   1s \rangle$	1.0000012	$\langle 2s   2s \rangle$	1.0000001
$\langle 1s   2s \rangle$	0.0000357	$\langle 2s   3s \rangle$	0.0000012
$\langle 1s   3s \rangle$	0.0000418	$\langle 2s   4s \rangle$	-0.0000037
$\langle 1s   4s \rangle$	0.0000272	$\langle 2s   5s \rangle$	-0.0000013
$\langle 1s   5s \rangle$	0.0000191	$\langle 2s   0.1s \rangle$	0.0000010
$\langle 1s   0.1s \rangle$	0.0000723	$\langle 2s   0.2s \rangle$	0.0000041
$\langle 1s   0.2s \rangle$	0.0001049	$\langle 2s   0.3s \rangle$	0.0000075
$\langle 1s   0.6s \rangle$	0.0002253	$\langle 2s   0.4s \rangle$	0.0000067
$\langle 1s   1.0s \rangle$	0.0003638	$\langle 2s   0.6s \rangle$	-0.0000066
$\langle 1s   1.6s \rangle$	0.0005253	$\langle 2s   1.0s \rangle$	0.0000007
$\langle 1s   2.0s \rangle$	0.0005626	$\langle 2s   2.0s \rangle$	-0.0000014
$\langle 1s   3.0s \rangle$	0.0005056	$\langle 2s   3.0s \rangle$	0.0000008
$\langle 1s   4.0s \rangle$	0.0003611	$\langle 2s   4.0s \rangle$	0.0000002
$\langle 1s   5.0s \rangle$	0.0002009	$\langle 2s   5.0s \rangle$	-0.0000001
$\langle 1s   6.0s \rangle$	0.0001000	$\langle 2s   6.0s \rangle$	-0.0000015
$\langle 1s   8.0s \rangle$	0.0000254	$\langle 2s   8.0s \rangle$	0.0000009

<sup>a</sup> Continuum states are normalized so that asymptotically  $P_k(r) = \sin(kr + (1/k)\ln 2kr + \delta)$ .

<sup>7</sup> I would like to thank Professor K. A. Brueckner for stressing the desirability of using a potential for excited states which has a physical basis and yields rapid convergence of the perturbation expansion.

TABLE II. Radial functions  $p_{2s}(r)$  for Be.

$r$	$P_{2s}^a(r)$	$P_{2s}^b(r)$	$r$	$P_{2s}^a(r)$	$P_{2s}^b(r)$
0.01	0.02569	0.02569	1.60	-0.58549	-0.58534
0.02	0.04936	0.04935	1.80	-0.61697	-0.61683
0.03	0.07110	0.07109	2.00	-0.62889	-0.62878
0.04	0.09104	0.09101	2.20	-0.62566	-0.62559
0.05	0.10926	0.10922	2.40	-0.61110	-0.61106
0.10	0.17771	0.17765	2.60	-0.58835	-0.58833
0.15	0.21536	0.21530	2.80	-0.55996	-0.55997
0.20	0.22985	0.22980	3.00	-0.52797	-0.52799
0.25	0.22700	0.22694	3.40	-0.45905	-0.45911
0.30	0.21123	0.21118	3.80	-0.39016	-0.39027
0.35	0.18596	0.18592	4.20	-0.32597	-0.32611
0.40	0.15381	0.15377	4.60	-0.26870	-0.26884
0.45	0.11681	0.11679	5.00	-0.21910	-0.21923
0.50	0.07655	0.07654	6.00	-0.12683	-0.12692
0.55	0.03428	0.03428	7.00	-0.07065	-0.07071
0.60	-0.00904	-0.00901	8.00	-0.03828	-0.03834
0.65	-0.05261	-0.05257	9.00	-0.02031	-0.02037
0.70	-0.09585	-0.09580	10.00	-0.01060	-0.01065
0.75	-0.13827	-0.13821	11.00	-0.00546	-0.00550
0.80	-0.17951	-0.17944	12.00	-0.00278	-0.00281
0.85	-0.21929	-0.21921	14.00	-0.00070	-0.00071
0.90	-0.25739	-0.25730	16.00	-0.00017	-0.00017
0.95	-0.29366	-0.29356	18.00	-0.00004	-0.00004
1.00	-0.32798	-0.32788			
1.20	-0.44492	-0.44479	$-\epsilon_{2s}$ (a.u.)	0.30942	0.30927
1.40	-0.52968	-0.52953			

<sup>a</sup> Calculated for this investigation. 1 a.u. = 27.21 eV.  
<sup>b</sup> Calculated by Roothaan, Sachs, and Weiss, Ref. 9.

the diagrams of Fig. 2 in calculations and to use the Hartree-Fock solutions for both  $1s$  and  $2s$  states. Bound and continuum states were calculated for  $l=0, 1$ , and  $2$ . The  $l=1$  and  $l=2$  states are orthonormal because they were all calculated with the same Hermitian potential and they are automatically orthonormal with respect to all  $l=0$  states. The  $2s$  Hartree-Fock (HF) state and all excited  $l=0$  states were calculated with the same Hermitian potential and are orthonormal. The only deviations from orthonormality in the basis set arise from the nonorthogonality of the HF  $1s$  state with excited  $l=0$  states. This nonorthogonality is not an error or an approximation as may be seen from the diagrams of Fig. 2. In actual calculations the nonorthogonality of the  $1s$  state and excited  $l=0$  states is expected

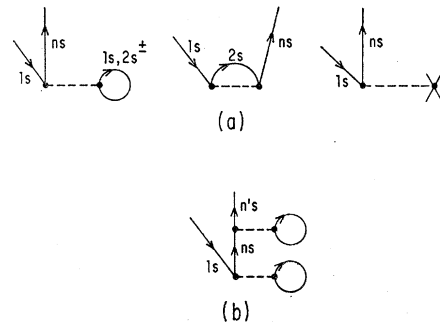


FIG. 2. (a) Single-particle corrections to the wave function  $\Phi_0$  in first order. When  $\varphi_{1s}$  is a Hartree-Fock orbital, these corrections vanish. When  $\varphi_{1s}$  is not determined by the Hartree-Fock potential, these terms and similar higher order terms as shown in (b) added to  $\Phi_0$  give effectively the Hartree-Fock result.

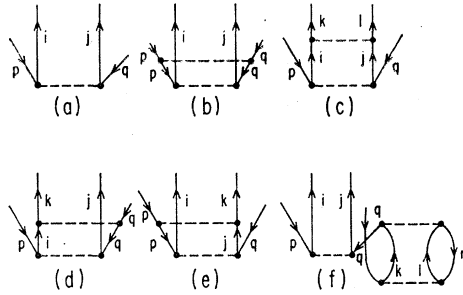


FIG. 3. Corrections to  $\Phi_0$  due to correlations among electrons in states  $p$  and  $q$ . (a) First-order term. (b) Diagonal hole-hole interaction. (c) Particle-particle interaction or ladder diagram. (d) and (e) are hole-particle interactions which represent the net effect of interactions of the particles in states  $i$  and  $j$  with all occupied unexcited states and with the potential  $V$ . It is assumed that  $i$  is calculated in the field of all unexcited states except  $p$  and  $j$  in the field of all but  $q$ . (f) Exclusion principle violating diagram arising from the linked cluster factorization.

to be very small. Overlap integrals of  $l=0$  states are given in Table I. All integrals were calculated by Simpson's rule. Orthogonality for the  $l=0$  states is quite good, even for the  $1s$  state with excited states for which, in principle, exact orthogonality is not expected. The lack of exact orthogonality between  $1s$  and  $2s$  states may be attributed to limits on the numerical accuracy of the HF  $1s$  state taken from the Kibartas and Yutsis solution.<sup>8</sup> All other states were calculated by the author's Hartree-Fock program which solves the following equation for  $\varphi_n$ .

$$-\frac{1}{2}\nabla^2\varphi_n(\mathbf{r}) - Z/r\varphi_n(\mathbf{r}) + \left(2\int d\mathbf{r}'\frac{\varphi_{1s}^*(\mathbf{r}')\varphi_{1s}(\mathbf{r}')}{|\mathbf{r}-\mathbf{r}'|} + \int d\mathbf{r}'\frac{\varphi_{2s}^*(\mathbf{r}')\varphi_{2s}(\mathbf{r}')}{|\mathbf{r}-\mathbf{r}'|}\right)\varphi_n(\mathbf{r}) - \int d\mathbf{r}'\frac{\varphi_{1s}^*(\mathbf{r}')\varphi_n(\mathbf{r}')}{|\mathbf{r}-\mathbf{r}'|}\varphi_{1s}(\mathbf{r}) = \epsilon_n\varphi_n(\mathbf{r}). \quad (13)$$

For Be,  $Z=4$ . The  $1s$  and  $2s$  states used in Eq. (13) were taken from Kibartas and Yutsis.<sup>8</sup> The  $2s$  state calculated by the author's program was in good agreement with the Kibartas solution. Comparison with the  $2s$  Be solution of Roothaan<sup>9</sup> is given in Table II. The very small disagreement in the fourth decimal place may not be attributed to a limit of accuracy for the author's program but is due to use of the Kibartas  $1s$  and  $2s$  states rather than Roothaan's in Eq. (13). In the calculations of this paper the most important perturbation terms are those involving  $2s$  states and excited  $l=1$  and  $l=2$  states.

### C. Summation of Diagrams

In order to obtain the corrections to  $\Phi_0$  due to correlations among a pair of electrons in states  $p$  and  $q$ , the

<sup>8</sup> V. V. Kibartas and A. P. Yutsis, Zh. Eksperim. i Teor. Fiz. 25, 264 (1953).

<sup>9</sup> C. C. J. Roothaan, L. M. Sachs, and A. W. Weiss, Rev. Mod. Phys. 32, 186 (1960).

diagrams of Fig. 3 are considered. For simplicity, states  $p$  and  $q$  have opposite spins. Figure 3(b) shows the diagonal part of the hole-hole interaction which violates the exclusion principle as discussed in K. In general, hole-hole nondiagonal interactions are quite small. The diagram of Fig. 3(c) shows a particle-particle interaction. It is assumed that the excited state  $i$  of Figs. 3(a) and 3(d) was calculated in the potential field of all unexcited states except for the state  $p$ . Interactions with the occupied unexcited states and with the potential combine to give the diagram (d). This diagram is analogous to that of Fig. 1(e). Similarly, it is assumed that the state  $j$  was calculated in the potential field of all unexcited states except for  $q$  and this gives Fig. 3(e). Diagrams shown in Fig. 1(d) are not included because excited states are now calculated in the field of  $N-1$  unexcited states. When  $i$  and  $j$  are bound-state diagrams (b), (c), (d), and (e) of Fig. 3 are largest for diagonal matrix elements. Diagram (c) is largest for  $i=k$ ,  $j=l$  and (d) and (e) are largest for  $i=k$  and  $j=k$ , respectively. The expression for the diagram of Fig. 3(a) is

$$(\epsilon_p + \epsilon_q - \epsilon_i - \epsilon_j)^{-1} \langle ij | v | pq \rangle. \quad (14)$$

For the diagonal interactions just described, the sum of diagrams 3(b) through 3(e) is given by

$$[(\epsilon_p + \epsilon_q - \epsilon_i - \epsilon_j)^{-1} (\langle pq | v | pq \rangle + \langle ij | v | ij \rangle - \langle iq | v | iq \rangle - \langle pj | v | pj \rangle)] (\epsilon_p + \epsilon_q - \epsilon_i - \epsilon_j)^{-1} \langle ij | v | pq \rangle. \quad (15)$$

When these diagonal interactions occur in the next order of perturbation theory the factor in brackets in Eq. (15) is repeated, and so the diagonal interactions give a geometric series which is readily summed to

$$D^{-1} \langle ij | v | pq \rangle, \quad (16)$$

where

$$D = (\epsilon_p + \epsilon_q - \langle pq | v | pq \rangle) - (\epsilon_i + \epsilon_j + \langle ij | v | ij \rangle - \langle iq | v | iq \rangle - \langle pj | v | pj \rangle). \quad (17)$$

When diagrams of the type shown in Fig. 3(f) are considered,  $D$  of Eq. (17) is further modified to<sup>10</sup>

$$D = [\epsilon_p + \epsilon_q - \langle pq | v | pq \rangle + E_{\text{corr}}(p, q) + E_{\text{corr}}(p, r \neq q) + E_{\text{corr}}(r \neq p, q)] - [\epsilon_i + \epsilon_j + \langle ij | v | ij \rangle - \langle iq | v | iq \rangle - \langle pj | v | pj \rangle - E_{\text{corr}}'(i, j)]. \quad (18)$$

The term  $E_{\text{corr}}(p, q)$  is the correlation energy among the two electrons in states  $p$  and  $q$ . The term  $E_{\text{corr}}(p, r \neq q)$  is the total correlation energy of an electron in state  $p$  from interactions with all unexcited states except for  $q$  and similarly for  $E_{\text{corr}}(r \neq p, q)$ . The term  $E_{\text{corr}}'(i, j)$  is the sum of all terms contributing to the total correlation energy in which either of the excited states  $i$  or  $j$  occurs and in which the hole states differ from  $p$  and  $q$ . Equa-

<sup>10</sup> In Ref. 5 diagrams of this type were shown to arise from the factorization of diagrams and they were labeled third class exclusion-principle-violating (EPV) diagrams. A more detailed analysis of such terms and their effects on Eq. (18) is given by H. Kelly, Phys. Rev. 134, A1450 (1964).

TABLE III. Dependence of matrix elements on  $n$ .<sup>a</sup>

$n$	$ \langle 2pn\bar{p} v 2s2s\rangle ^2$	$n^3 \langle 2pn\bar{p} v 2s2s\rangle ^2$	$n$	$ \langle nd r^2 2s\rangle ^2$	$n^3 \langle nd r^2 2s\rangle ^2$
2	$3.644\times 10^{-2}$	0.2915	3	$5.169\times 10^1$	1395.6
3	$2.569\times 10^{-3}$	0.0694	4	$1.604\times 10^1$	1026.3
4	$7.371\times 10^{-4}$	0.0472	5	$7.022\times 10^0$	877.8
5	$3.171\times 10^{-4}$	0.0396	6	$3.724\times 10^0$	804.3
6	$1.667\times 10^{-4}$	0.0360	7	$2.223\times 10^0$	762.5
7	$9.889\times 10^{-5}$	0.0339	8	$1.438\times 10^0$	736.2
8	$6.364\times 10^{-5}$	0.0326	9	$9.857\times 10^{-1}$	718.6
10			10	$7.062\times 10^{-1}$	706.2
$n$	$ \langle np r 2s\rangle ^2$	$n^3 \langle np r 2s\rangle ^2$	$n$	$ \langle nd r^{-2} 2s\rangle ^2$	$n^3 \langle nd r^{-2} 2s\rangle ^2$
2	$7.849\times 10^0$	62.794	3	$7.317\times 10^{-5}$	$1.976\times 10^{-3}$
3	$1.480\times 10^{-2}$	0.400	4	$4.099\times 10^{-5}$	$2.623\times 10^{-3}$
4	$1.299\times 10^{-2}$	0.831	5	$2.328\times 10^{-5}$	$2.910\times 10^{-3}$
5	$7.446\times 10^{-3}$	0.931	6	$1.419\times 10^{-5}$	$3.064\times 10^{-3}$
6	$4.443\times 10^{-3}$	0.960	7	$9.176\times 10^{-6}$	$3.147\times 10^{-3}$
7	$2.823\times 10^{-3}$	0.968	8	$6.259\times 10^{-6}$	$3.204\times 10^{-3}$
8	$1.894\times 10^{-3}$	0.970	9	$4.437\times 10^{-6}$	$3.235\times 10^{-3}$
10			10	$3.284\times 10^{-6}$	$3.284\times 10^{-3}$
$n$	$ \langle np r^{-2} 2s\rangle ^2$	$n^3 \langle np r^{-2} 2s\rangle ^2$	$n$	$ \langle nd r^2 1s\rangle ^2$	$n^3 \langle nd r^2 1s\rangle ^2$
2	$1.830\times 10^{-2}$	0.1464	3	$9.711\times 10^{-5}$	$2.622\times 10^{-3}$
3	$1.711\times 10^{-3}$	0.0462	4	$5.707\times 10^{-5}$	$3.653\times 10^{-3}$
4	$5.260\times 10^{-4}$	0.0337	5	$3.304\times 10^{-5}$	$4.130\times 10^{-3}$
5	$2.327\times 10^{-4}$	0.0291	6	$2.030\times 10^{-5}$	$4.385\times 10^{-3}$
6	$1.241\times 10^{-4}$	0.0268	7	$1.323\times 10^{-5}$	$4.537\times 10^{-3}$
7	$7.424\times 10^{-5}$	0.0255	8	$9.051\times 10^{-6}$	$4.634\times 10^{-3}$
8	$4.804\times 10^{-5}$	0.0246	9	$6.446\times 10^{-6}$	$4.699\times 10^{-3}$
10			10	$4.746\times 10^{-6}$	$4.746\times 10^{-3}$
$n$	$ \langle np r 1s\rangle ^2$	$n^3 \langle np r 1s\rangle ^2$	$n$	$\langle 2s r^2 nd\rangle\langle nd r^{-3} 2s\rangle$	$n^3\langle 2s r^2 nd\rangle\langle nd r^{-3} 2s\rangle$
2	$2.515\times 10^{-2}$	0.2012	3	$6.150\times 10^{-2}$	1.660
3	$4.774\times 10^{-3}$	0.1289	4	$2.564\times 10^{-2}$	1.641
4	$1.791\times 10^{-3}$	0.1146	5	$1.279\times 10^{-2}$	1.598
5	$8.637\times 10^{-4}$	0.1080	6	$7.268\times 10^{-3}$	1.570
6	$4.819\times 10^{-4}$	0.1041	7	$4.517\times 10^{-3}$	1.549
7	$2.960\times 10^{-4}$	0.1015	8	$3.000\times 10^{-3}$	1.536
8	$1.947\times 10^{-4}$	0.0997	9	$2.091\times 10^{-3}$	1.525
10			10	$1.523\times 10^{-3}$	1.523

<sup>a</sup> Only radial parts of matrix elements are given.

tion (18) is the two-particle energy for states  $p$  and  $q$  minus the approximate two-particle energy for states  $i$  and  $j$ . In the first bracket, subtraction of  $\langle pq|v|pq\rangle$  from  $\epsilon_p + \epsilon_q$  corrects for the fact that each single-particle state was calculated in the potential field of the other and so the interaction of  $p$  with  $q$  was counted twice. Then  $\epsilon_p + \epsilon_q - \langle pq|v|pq\rangle$  is the Hartree-Fock energy for the pair  $pq$ .  $E_{\text{corr}}(p, q)$  accounts for higher order interactions of  $p$  with  $q$  and  $E_{\text{corr}}(p, r \neq q)$  and  $E_{\text{corr}}(r \neq p, q)$  account for the higher order interactions of  $p$  and  $q$  with the other unexcited states since these interactions are not included in the HF calculation of  $\epsilon_p$  and  $\epsilon_q$ . In the second bracket,  $\langle ij|v|ij\rangle$  accounts for the interaction of  $i$  with  $j$  and  $-\langle iq|v|i\rangle$  corrects for the fact that  $i$ , which was calculated with interactions with  $q$ , does not interact with  $q$  which is now unoccupied. The term  $-\langle pj|v|pj\rangle$  corrects similarly for state  $j$ . The first five terms of the second bracket of Eq. (18) then give essentially the HF energy of the excited pair  $ij$ . The term  $-E_{\text{corr}}(i, j)$  does not give correlations between  $i$  and  $j$  but accounts for the fact that all correlations among unexcited pairs which involve excitations into states  $i$  or  $j$  are eliminated by the Pauli principle when  $p$  and  $q$  are excited into  $i$  and  $j$ . Although

the discussion of this section has treated bound excited states, it is readily extended to continuum states as shown previously.<sup>5,11</sup> In numerical applications the nondiagonal higher order terms are calculated but they converge rapidly.

### III. SUMS OVER BOUND EXCITED STATES

In later sections the BG theory is used to calculate the correlation energy among  $2s$  electrons and other properties for Be. In using BG perturbation theory, it is necessary to sum over all excited states. When the continuum is considered, the sums are readily evaluated by numerical integrations as shown in K. It is not obvious that the sums over bound states may be handled so simply, however. One often includes just the first few bound states and assumes that the remaining contributions are small. This is probably reasonable in many cases; however, it is preferable to sum over all bound excited states and this is now shown to be feasible. In the numerical work reported here it was found that matrix elements such as  $\langle mpn\bar{p}|v|2s2s\rangle$  are proportional to  $n^{-3/2}$  for fixed  $m$  as  $n$  becomes large. This behavior

<sup>11</sup> H. P. Kelly and A. M. Sessler, Phys. Rev. **132**, 2091 (1963)

is expected to hold true for other operators and for other atoms when the asymptotic potential is Coulombic as in this case. The explanation lies in the fact that  $\varphi_{2s}$  lies much closer to the nucleus than  $\varphi_{np}$  for  $n$  large. When we compute  $\varphi_{n+1p}$  there is very little change in the single-particle energy and the behavior of  $\varphi_{n+1p}$  is very close to that of  $\varphi_{np}$  (except for normalization) in the region of space where  $\varphi_{2s}$  is substantially nonzero. The principal change in the matrix element in going from  $n$  to  $n+1$  then is due to the change in the normalization factors.

It is shown, for example, by Bethe and Salpeter<sup>12</sup> that for hydrogen-like atoms the behavior of the eigenfunctions for large principal quantum number  $n$  is

$$R_{nl} \approx 2 \left( \frac{Z}{n} \right)^{3/2} \frac{(2Zr)^l}{(2l+1)!} \left[ 1 - \frac{2rZ}{2l+2} + \dots \right]. \quad (19)$$

The potential used in Eq. (13) is asymptotically Coulombic and since  $\varphi_{np}$  for large  $n$  is located mainly in the asymptotic region of the potential, it is expected that the normalization of  $\varphi_{np}$  should contain the factor  $n^{-3/2}$  as does that of hydrogen. The numerical checks on this rule are given in Table III. When the product  $n^3$  times matrix element squared has not completely reached its asymptotic value, a curve may be drawn to estimate the higher values and the limit. In perturbation theory calculations we consider terms of the form

$$\sum_{m=2}^{\infty} \sum_{n=2}^{\infty} |\langle m p n p | v | 2s 2s \rangle|^2 D^{-1}, \quad (20)$$

where  $D$  is given by Eq. (18). The double summation presents no essential complication in the following discussion. As  $n$  in Eq. (20) becomes large,  $D$  approaches a constant value. This allows us to carry out the summations of Eq. (20). For example, for fixed  $m$  we might carry out the sum from  $n=2$  to  $n=8$  by explicit calculation of the terms. Then from  $n=9$  to approximately  $n=15$  we would calculate terms by using the  $n^{-3}$  rule for the matrix elements squared and we would make the necessary extrapolations to obtain accurate denominators. For example,  $\epsilon_{np} \propto n^{-2}$ . The remainder of the sum is obtained to a good approximation from

$$C \int_{N_f+1}^{\infty} n^{-3} dn = C / [2(N_f+1)^2], \quad (21)$$

where  $N_f$  is the last  $n$  value calculated by discrete summation and

$$C = \lim_{n \rightarrow \infty} n^3 |\langle m p n p | v | 2s 2s \rangle|^2 D^{-1}. \quad (22)$$

For greater accuracy we may also use  $\zeta(3)$  where  $\zeta(s)$

<sup>12</sup> H. A. Bethe and E. E. Salpeter, *Quantum Mechanics of One- and Two-Electron Systems* (Academic Press Inc., New York, 1957), p. 18.

TABLE IV. Numerical values in a.u. for  $D$  of Eq. (23) and for excitation matrix element.

$\epsilon_{2s}$	-0.30942
$\epsilon_{2p}$	-0.17951
$E_{\text{corr}}(2s, 2s)$	-0.0439
$4E_{\text{corr}}(2s; 1s)$	-0.00497
$\langle 2s 2s   v   2s 2s \rangle$	0.34331
$\langle 2p 2p   v   2p 2p \rangle^a$ ( $m_l = \pm 1$ )	0.28652
$\langle 2p 2p   v   2p 2p \rangle$ ( $m_l = 0$ )	0.30180
$\langle 2p 2s   v   2p 2s \rangle$	0.30867
$\langle 2p 2p   v   2s 2s \rangle^b$	0.0636315

<sup>a</sup> One  $2p$  state has  $m_l = +1$  and the other  $m_l = -1$ .

<sup>b</sup> This term is negative for  $m_l = \pm 1$  and positive for  $m_l = 0$ .

is the zeta function of Riemann<sup>13</sup> given by

$$\zeta(s) = \sum_{n=1}^{\infty} 1/n^s.$$

In the calculations of the next sections  $N_f$  is typically 15. This procedure may be carried out to any desired accuracy by calculation of a sufficient number of excited states. The sums of Eq. (20) must be repeated for different values of  $m$  and an extrapolation made for  $m \rightarrow \infty$  just as for  $n$ .

#### IV. Be CORRELATION ENERGY FOR 2s ELECTRONS

In K it was found that almost all the contribution to  $2s-2s$  correlations in Be came from excitations into  $l=1$  states. This calculation has been again made using BG theory but with the set of single-particle states of Eq. (13). Diagonal terms beyond second order are included in the "second-order" calculation by using the denominator  $D$  of Eq. (18). The nondiagonal third-order and higher terms are also calculated. The states  $p$  and  $q$  in Eq. (18) are now the Hartree-Fock  $2s$  states of Be. The term  $E_{\text{corr}}(2s, 2s)$  was found to be  $-0.0439$  atomic units (a.u.) in K. The terms  $E_{\text{corr}}(p, r \neq q) + E_{\text{corr}}(r \neq p, q)$  give the total correlation energy between the  $2s$  and  $1s$  shells which was calculated to be  $-0.00497$  a.u. in K. One a.u. = 27.21 eV. Most of the contribution to the  $2s$  correlation energy will be shown to come from excitations into  $2p$  states. The term  $E_{\text{corr}}'(i, j)$  is the contribution to the correlation energy among  $1s$  electrons when at least one of the excited states coincides with  $i$  or  $j$ . For  $2p$  excitations  $E_{\text{corr}}'$  was calculated to be  $-0.00027$  a.u. This is quite small relative to the other terms in Eq. (18) so  $E_{\text{corr}}'(i, j)$  is omitted. When both  $2s$  electrons are excited into  $2p$  states

$$D = \epsilon_{2s} + \epsilon_{2s} - \epsilon_{2p} - \epsilon_{2p} + E_{\text{corr}}(2s, 2s) + 4E_{\text{corr}}(2s, 1s) - \langle 2s 2s | v | 2s 2s \rangle - \langle 2p 2p | v | 2p 2p \rangle + 2 \langle 2p 2s | v | 2p 2s \rangle. \quad (23)$$

The numerical values are given in Table IV. Although the notation has so far been suppressed, excited states

<sup>13</sup> E. T. Whittaker and G. N. Watson, *Modern Analysis* (Cambridge University Press, Cambridge, 1927), Chap. XIII, p. 265.

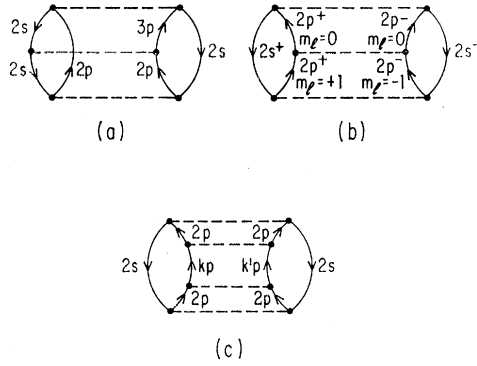


FIG. 4. Changes in excited states due to nondiagonal interactions. (a) Hole-particle interaction. (b) Particle-particle interaction. (c) Two nondiagonal interactions.

are labeled by  $m_l$  and  $m_s$  in addition to  $n$  and  $l$ . The angular factors for matrix elements, which may be obtained from Condon and Shortley,<sup>14</sup> affect  $\langle 2p2p|v|2p2p\rangle$  differently according to the  $m_l$  values of the  $2p$  excited states. When we write the sums over  $m_l$  explicitly,

$$E_{\text{corr}}(2s, 2s \rightarrow mp, np) = 2|\langle mpnp|v|2s2s\rangle|^2 / D(m_l = \pm 1) + |\langle mpnp|v|2s2s\rangle|^2 / D(m_l = 0). \quad (24)$$

The results of Eq. (24) are given in Table V for  $m=2$  and  $n$  variable.

The sums over continuum states are readily performed as described in K. In the following term one excitation is into a bound state and one into the continuum

$$\sum_k E_{\text{corr}}(2s, 2s \rightarrow np, kp) = -\frac{2}{\pi} \int_0^\infty dk |\langle 2s2s|v|npkp\rangle|^2 / D(k), \quad (25)$$

where

$$D(k) = \epsilon_{2s} + \epsilon_{2s} - \epsilon_{np} - k^2/2 + E_{\text{corr}}(2s, 2s) + 4E_{\text{corr}}(2s, 1s) - \langle 2s2s|v|2s2s\rangle + \langle np2s|v|np2s\rangle. \quad (26)$$

TABLE V. Bound-state contributions to  $E_{\text{corr}}$  involving  $2p$  states.

$n$	$E_{\text{corr}}(2s2s \rightarrow 2pnp)$ in a.u.
2	-0.037244
3	-0.003781
4	-0.001011
5	-0.000423
6	-0.000219
7	-0.000129
8	-0.000082
9	-0.000056
10	-0.000040
$\sum_{n=11}^{\infty}$	-0.000170
Total	-0.04316

<sup>14</sup> E. U. Condon and G. H. Shortley, *The Theory of Atomic Spectra* (Cambridge University Press, Cambridge, England, 1957), p. 178.

TABLE VI. Diagonal contributions to  $E_{\text{corr}}(2s, 2s)$  from  $p$  states.<sup>a</sup>

Lowest state <sup>b</sup>	Sum of bound states <sup>c</sup>	Continuum states <sup>d</sup>	Bound + continuum
$2p$	$-4.3155 \times 10^{-2}$	$-3.804 \times 10^{-3}$	$-4.6959 \times 10^{-2}$
$3p$	$-3.003 \times 10^{-4}$	$-5.225 \times 10^{-4}$	$-8.228 \times 10^{-4}$
$4p$	$-3.89 \times 10^{-5}$	$-1.794 \times 10^{-4}$	$-2.183 \times 10^{-4}$
$5p$	$-9.61 \times 10^{-6}$	$-8.210 \times 10^{-5}$	$-9.171 \times 10^{-5}$
$6p$	$-3.36 \times 10^{-6}$	$-4.456 \times 10^{-5}$	$-4.792 \times 10^{-5}$
$7p$	$-1.44 \times 10^{-6}$	$-2.693 \times 10^{-5}$	$-2.837 \times 10^{-5}$
$8p$	$-7.10 \times 10^{-7}$	$-1.754 \times 10^{-5}$	$-1.825 \times 10^{-5}$
$9p$	$-3.75 \times 10^{-7}$	$-1.209 \times 10^{-5}$	$-1.247 \times 10^{-5}$
$10p$	$-2.16 \times 10^{-7}$	$-8.680 \times 10^{-6}$	$-8.900 \times 10^{-6}$
$11p$	$-1.33 \times 10^{-7}$	$-6.440 \times 10^{-6}$	$-6.570 \times 10^{-6}$
$12p$	$-9.0 \times 10^{-8}$	$-4.910 \times 10^{-6}$	$-5.000 \times 10^{-6}$
$\sum_{n=13}^{\infty} np$	$-4.14 \times 10^{-7}$	$-2.470 \times 10^{-5}$	$-2.510 \times 10^{-5}$
Bound+continuum total:			$-4.8245 \times 10^{-2}$
Continuum-continuum states:			$-1.6827 \times 10^{-3}$
Diagonal total			$-4.9928 \times 10^{-2}$

<sup>a</sup> All energies are in a.u. Second-order and only diagonal higher order bound-state contributions are included. See Eq. (24). Sums over  $m_l$  have been made.

<sup>b</sup> One of the two excited states has this quantum number. The other state has a principal quantum number greater than or equal to this.

<sup>c</sup> The sum is over all bound excited states with principal quantum number greater than or equal to that at the left. In the first row the sum runs from  $2p$  to  $\infty$ . In second row the sum runs from  $3p$  to  $\infty$ , etc.

<sup>d</sup> Hole-particle and particle-particle interactions are included.

Note that diagonal bound-state contributions are included. The continuum particle interaction with the  $2s$  hole is treated as in K and similarly for the particle-particle interaction. That is, we consider

$$a_{np}(k) = -\frac{2}{\pi} \int_0^\infty dk' \langle 2sk|v|2sk'\rangle D^{-1}(k') \times \langle npk'|v|2s2s\rangle \langle npk|v|2s2s\rangle^{-1} \quad (27)$$

and

$$t_{np}(k) = -\frac{2}{\pi} \int_0^\infty dk' \langle npk|v|npk'\rangle D(k')^{-1} \times \langle npk'|v|2s2s\rangle \langle npk|v|2s2s\rangle^{-1}. \quad (28)$$

In Eq. (28) there is also a sum over  $m_l$ . As found previously in K for two continuum excitations, both  $a_{np}(k)$  and  $t_{np}(k)$  were almost constant, with a very small dependence on  $k$ . The ladder or particle-particle interactions and the continuum particle-hole interactions are then summed by multiplying Eq. (25) by the factor

$$(1 - a_{np}(k) - t_{np}(k))^{-1}, \quad (29)$$

where an average value for  $k$  is used. The term  $t_{np}$  differs by 4% for  $np(m_l = \pm 1)$  and  $np(m_l = 0)$ .

For  $n=2$ ,  $a_{2p}(0.4) = 0.3385$ ,  $t_{2p}(0.4) = 0.323$  ( $m_l = \pm 1$ ), and  $t_{2p}(0.4) = 0.337$  ( $m_l = 0$ ). The factor of Eq. (29) is then 1.0109, a small correction.

Contributions to the  $2s$  correlation energy from the various excited  $l=1$  states are given in Table VI. The principal contribution is seen to come from  $2p$  excitations.

Some typical nondiagonal terms are given in Fig. 4. Changes from one continuum state to another have

already been included in Table VI. All calculations are made with the shifted denominator of Eq. (18). All nondiagonal terms with a significant contribution to  $E_{\text{corr}}(2s, 2s)$  are listed in Table VII. The total contributions of Tables VI and VII are added to give  $E_{\text{corr}}(2s, 2s) \times (l=1) = -0.04357$  a.u. In the previous calculations of K,  $E_{\text{corr}}(2s, 2s)(l=1)$  was found to be  $-0.04256$  a.u. The value calculated here is believed to be a much more accurate result than the calculation of K. If the new value for  $E_{\text{corr}}(2s, 2s)(l=1)$  is added to the other contributions to the total correlation energy calculated in K, the total correlation energy of Be is changed from  $-0.091$  to  $-0.092$  a.u. which improves agreement with the value  $-0.0953$  a.u. deduced from experiment.

## V. POLARIZABILITIES AND SHIELDING FACTORS

### A. Dipole Polarizability for Be

An atom perturbed by an external charge  $Z'$  becomes polarized; and the effect of the external electric field on the atom depends upon the atomic dipole polarizability  $\alpha_a$ . An extensive discussion of atomic polarizabilities and shielding factors has been given by Dalgarno<sup>15</sup> and his notation is used in this section.

The unperturbed Hamiltonian is

$$H = -\sum_{i=1}^N \left( \frac{\nabla_i^2}{2} + \frac{Z}{r_i} \right) + \sum_{i<j}^N |\mathbf{r}_i - \mathbf{r}_j|^{-1}. \quad (30)$$

Atomic units are used in all formulas. The ground-state wave function  $\Psi_0$  satisfies<sup>16</sup>

$$(H - E)\Psi_0 = 0. \quad (31)$$

TABLE VII. Nondiagonal terms in  $E_{\text{corr}}(2s, 2s)$  for  $l=1$ .<sup>a</sup>

$2p2p \rightarrow 2p2p^b$	$4.058 \times 10^{-3}$
$\sum_{n=3}^{\infty} (2p2p \rightarrow 2pn p)$	$2.016 \times 10^{-4}$
$2p2p \rightarrow 2pkp$	$-2.655 \times 10^{-4}$
$\sum_{n=3}^{\infty} (2p2p \rightarrow 3pn p)$	$2.45 \times 10^{-4}$
$2p2p \rightarrow 3pkp$	$4.11 \times 10^{-4}$
$\sum_{n=4}^{\infty} (2p2p \rightarrow np \binom{m p}{k p})^c$	$3.66 \times 10^{-4}$
$2p2p \rightarrow kpkp$	$1.399 \times 10^{-3}$
Nondiagonal total	$6.355 \times 10^{-3}$

<sup>a</sup> Hole-particle diagrams and ladder diagrams are included.

<sup>b</sup> This includes  $2p^+(m_i = \pm 1)2p^-(m_i = \mp 1) \rightarrow 2p^+(m_i = \pm 1)2p^-(m_i = \pm 1)2p^+(m_i = \pm 1)2p^-(m_i = \mp 1) \leftrightarrow 2p^+(m_i = 0)2p^-(m_i = 0)$ .

<sup>c</sup> This includes sum  $m \geq n$ .

<sup>15</sup> A. Dalgarno, *Advan. Phys.* **11**, 281 (1962).

<sup>16</sup> Note that  $\Psi_0$  is unperturbed with respect to interactions with the external charge  $Z'$ . However,  $\Psi_0$  includes correlation effects and is perturbed with respect to the Hartree-Fock solution.

The interaction potential between the external charge  $Z'$  at  $\mathbf{r}'$  and the atom is given by

$$V_{\text{ext}} = -Z' \sum_{i=1}^N \sum_{k=1}^{\infty} (r_i^k / r'^{k+1}) P_k(\cos \theta_i), \quad (32)$$

where the polar axis has been chosen along the line between the nucleus and  $\mathbf{r}'$  and the constant, spherically symmetric part of  $V_{\text{ext}}$  has been omitted. The perturbed wave function

$$\Psi = \Psi_0 + Z' \sum_{k=1}^{\infty} \Psi_1^{(k)} / r'^{k+1} + O(Z'^2). \quad (33)$$

The dipole polarizability is

$$\alpha_a = 2 \langle \Psi_0 | \sum_{i=1}^N r_i P_1(\cos \theta_i) | \Psi_1^{(1)} \rangle / \langle \Psi_0 | \Psi_0 \rangle, \quad (34)$$

where  $Z'$  is assumed small. The wave function  $\Psi_1^{(1)}$  then is the function  $\Psi_0$  perturbed once by the term  $-U_1$  where

$$U_k = \sum_{i=1}^N r_i^k P_k(\cos \theta_i). \quad (35)$$

In our case the function  $\Psi_0$  is not known at the outset; so we start from the Hartree-Fock  $\Phi_0$  and use BG theory to calculate  $\Psi$ .

The perturbation is

$$H' = \sum_{i<j}^N |\mathbf{r}_i - \mathbf{r}_j|^{-1} - \sum_{i=1}^N V_i - Z' \sum_{k=1}^{\infty} U_k / r'^{k+1}. \quad (36)$$

The BG linked cluster result is derived as usual<sup>2</sup> and

$$\Psi = \sum_L \left( \frac{1}{E_0 - H_0} \right)^n \Phi_0, \quad (37)$$

where  $\sum_L$  indicates that we sum over all linked terms.<sup>2</sup> The function  $\Psi_0$  is given by the sum of all terms of  $\Psi$  in which there are no interactions involving  $U_k$ . The term  $\Psi_1^{(1)}$  is the sum of all terms of  $\Psi$  in which  $-U_1$  acts once and only once,  $Z'/r'^2$  being factored out.  $\Psi_0$  obtained from Eq. (37) is not normalized to unity. However, in the numerator of Eq. (34) we may factor the disconnected terms into a product of terms involving  $U_1$  times all other terms. If we neglect the exclusion principle, the second factor is  $\langle \Psi_0 | \Psi_0 \rangle$  and cancels the denominator. This factorization proceeds as in the derivation of the linked cluster result. However, the exclusion principle must be considered in this factorization and it will be shown to have a significant effect for small systems.

The terms contributing to Eq. (34) may be represented by diagrams as in Fig. 5. The ordering of interactions from the bottom to the top of the diagram corresponds to interactions proceeding from right to left in Eq. (34). The interaction lines labeled DP for dipole

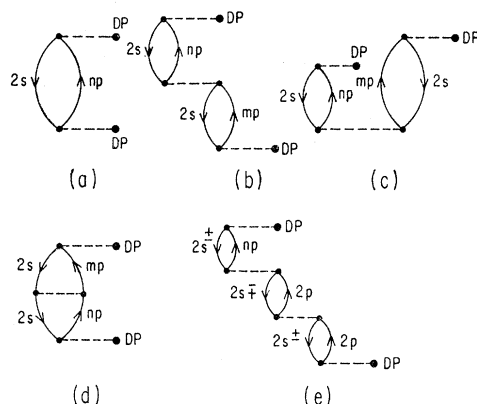


FIG. 5. Lowest order terms contributing to the dipole polarizability  $\alpha_d$ . The interaction labeled DP refers to the dipole polarizability operator  $r \cos\theta$ . (a) Second-order term. (b) and (c) are third-order terms with one correlation interaction. There is also the term obtained by inverting (c). (d) Hole-particle interaction diagram which does not occur when the single-particle states are calculated as in this paper. (e) Fourth-order diagram which is an iteration of the diagram (b).

polarizability indicate interactions through the operator  $U_1$ . The diagrams are calculated by the usual perturbation theory rules<sup>2</sup> and multiplied by  $-2$  to give  $\alpha_d$ . The factor 2 comes from Eq. (34) and  $(-1)$  from Eq. (36). The lowest order contribution to  $\alpha_d$  is positive; it is shown in Fig. 5(a) and has the value

$$\alpha_d(2s \rightarrow np) = -4 |\langle 2s | r \cos\theta | np \rangle|^2 / (\epsilon_{2s} - \epsilon_{np}). \quad (38)$$

Equation (38) includes a factor 2 because there are two  $2s$  electrons. Transitions to continuum states are given by

$$\sum_k \alpha_d(2s \rightarrow kp) = -\frac{8}{\pi} \int_0^\infty dk |\langle 2s | r \cos\theta | kp \rangle|^2 / (\epsilon_{2s} - k^2/2), \quad (39)$$

where the continuum states are normalized so that

$$P_k(r) = \sin(kr + (1/k) \ln 2kr + \delta) \quad (40)$$

as  $r \rightarrow \infty$  and  $\sum_k = (2/\pi) \int_0^\infty dk$  as shown in K. The

TABLE VIII. Dipole polarizability in second order.<sup>a</sup>

$n$	$\alpha_d(2s \rightarrow np) \text{ \AA}^3$	$n$	$\alpha_d(1s \rightarrow np) \text{ \AA}^3$
2	11.9371	2	0.001091
3	0.01213	3	0.000202
4	0.00939	4	0.0000753
5	0.00513	5	0.0000362
6	0.00298	6	0.0000202
7	0.00187	7	0.0000124
8	0.00124	8	0.0000081
$\sum_{n=9}^\infty$	0.00393	$\sum_{n=9}^\infty$	0.0000257
continuum	0.17049	continuum	0.005848
2s total	12.1443 $\text{\AA}^3$	1s total	0.007319 $\text{\AA}^3$

<sup>a</sup> 1  $\text{\AA}^3 = 10^{-24} \text{ cm}^3$ .

second-order contribution to  $\alpha_d$  from  $1s$  electrons is obtained by replacing  $2s$  by  $1s$  in Eqs. (38) and (39). Numerical results for  $\alpha_d$  in second order are given in Table VIII. The validity of the  $n^{-3}$  rule for  $|\langle 2s | r \cos\theta | np \rangle|^2$  may be checked in Table III. It is interesting to note that almost the entire contribution to  $\alpha_d$  comes from  $2p$  excited states and that excitations of  $1s$  electrons contribute negligibly. The second-order  $\alpha_d$  is  $12.15 \text{ \AA}^3$  as compared with  $4.54 \text{ \AA}^3$  obtained by Kelly and Taylor<sup>17</sup> in a second-order calculation using the set of Hartree-Fock states described in K in which all excited states are in the continuum. It was pointed out<sup>17</sup> that this second-order calculation is equivalent to the uncoupled Hartree-Fock approximation of Dalgarno.<sup>15</sup> In higher order calculations using this continuum set it is necessary to calculate the diagram of Fig. 5(d) and higher iterations. This type of diagram was called a second class EPV diagram in K. It arises from the fact that for this set the interactions of an excited particle with the Hartree-Fock potential do not cancel the interactions with the occupied unexcited states. This is the analog of Fig. 1(d).

In K these diagrams were found to be comparable in size to the second-order term and of the same sign. In the calculations of this paper the single-particle states were calculated so that interactions of excited states with the potential are canceled by interactions with the occupied unexcited states when there is only a single  $2s$  excitation. Another way to look at this problem is to note that all terms of the type of Fig. 5(d) have been summed and need no longer be considered when the states of this paper are used. Since these terms are all of the same sign as the second-order term, it is understandable that the second order result of this paper should be much larger than that reported in KT.

The third order terms of Figs. 5(b) and (c) which reduce the second-order result are found to be large. This is expected since they differ from the second-order term by one  $l=1$  correlation interaction, and in Sec. IV

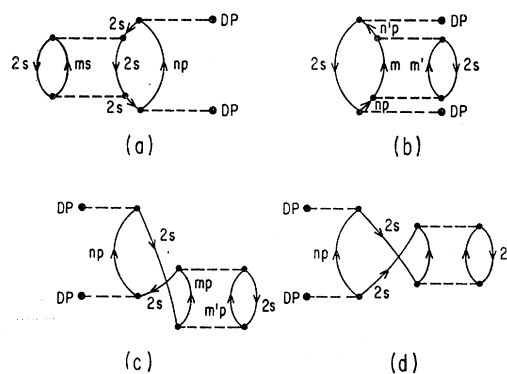


FIG. 6. Fourth-order diagrams which modify single-particle excitations. Diagrams (a), (c), and (d) are rearrangement diagrams discussed in Ref. 18.

<sup>17</sup> H. P. Kelly and H. S. Taylor, J. Chem. Phys. **40**, 1478 (1964), hereafter referred to as KT.

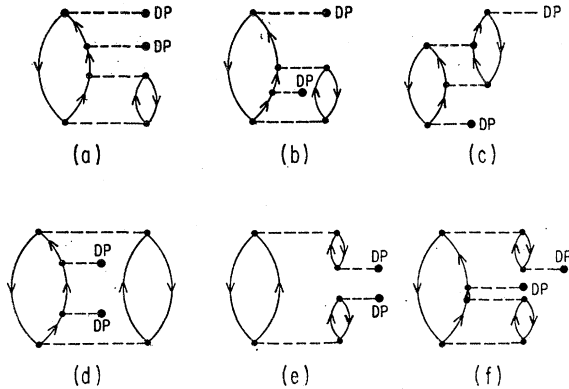


FIG. 7. Basic fourth-order diagrams contributing to the dipole polarizability  $\alpha_d$  are given by diagrams (a), (b), (c), (d), and (e). Diagrams (a), (b), and (f) may be inverted. In diagrams (b) and (d) the first DP interaction may also occur on the other particle line. A fifth-order diagram modifying (a) is given by (f). Similar diagrams modify (b) and (c).

these correlations were large. It is desirable to include as many higher order effects as possible when the basic third-order diagrams are calculated. This is achieved by first considering modifications to the single-particle excitations shown in Figs. 6(a), (b), (c), and (d). These modifications will be shown to be included by an effective shift in the energy denominators for single-particle excitations and they are found to be small compared to other effects. The modification which is numerically largest is shown in Fig. 5(e). That is, whenever we have a single-particle excitation we include all correlation interactions which interchange the excited and unexcited  $2s$  electrons. Due to the dominance of excitations into  $2p$  states as seen from Tables II and VI, it is possible to sum exactly the principal part of this modification by considering the geometrical series

$$MF = 1 + (\langle 2p2s | v | 2s2p \rangle / (\epsilon_{2s} - \epsilon_{2p} + d)) + \dots \\ = [1 - \langle 2p2s | v | 2s2p \rangle / (\epsilon_{2s} - \epsilon_{2p} + d)]^{-1}. \quad (41)$$

The term  $d$  is due to the modifications of Fig. 6. Whenever there is a single excitation into the state  $2p$ , the term is multiplied by  $MF$ . In Fig. 5(b) for  $m=2$  and  $n \neq 2$ , we multiply by  $MF$  and have included all diagrams like that of Fig. 5(e) to all orders. If we multiply the diagram of Fig. 5(a) by  $MF$  then we must be careful not to include  $n=m=2$  in Fig. 5(b) as this is already included in  $MF$ . In these calculations,  $MF=0.696$ . When the diagram of Fig. 5(c) is calculated, the denominator  $D$  of Eq. (18) is used to account for higher correlation effects. The nondiagonal terms discussed in Sec. III must also be included. When  $m=2$ , this diagram is multiplied by  $MF$ . The inverted diagram is numerically identical.

Modifications due to the diagrams of Fig. 6 are now considered. Diagrams (a), (c), and (d) are "rearrangement" diagrams discussed by Brueckner and Goldman.<sup>18</sup>

<sup>18</sup> K. A. Brueckner and D. T. Goldman, Phys. Rev. **117**, 207 (1960).

Diagrams (c) and (d) result from the linked cluster factorization and may be added to give the negative product of the second-order term for  $\alpha_d$  and the second-order correlation energy term. Higher order diagrams like (c) and (d) give additional factors of correlation energy terms and the result is a geometrical series which may be summed to give the second-order term for  $\alpha_d$  with the shifted denominator<sup>10</sup>

$$D = \epsilon_{2s} - \epsilon_{2p} + E_{\text{corr}}(2s, 2s) + 2E_{\text{corr}}(2s, 1s). \quad (42)$$

Calculations of 6(a) and (b) were made for  $n=n'=2$  as  $2p$  excitations are dominant. The ratio of diagrams (a) and (b) to the second-order diagram of  $\alpha_d$  establishes the ratio of terms in a geometric series which is also summed to give a shifted denominator. In calculating (b),  $m$  and  $m'$  are the possible excited bound and continuum states consistent with the rules for allowed angular momenta of single-particle states in Coulomb matrix elements.<sup>14</sup> That is, we may have  $mp m's$ ,  $mp m'd$ ,  $md m'p$ , etc. In calculating 6(b), only  $s$ ,  $p$ , and  $d$  states were considered. The shift in Eq. (42) due to diagrams like 6(c) and (d) is  $-0.0465$  a.u. However, this number is largely canceled by the shift due to diagrams like 6(a) and (b) and the net shift is only  $-0.0156$  a.u. For comparison,  $\epsilon_{2s} - \epsilon_{2p} = -0.1299$  a.u. Also, this effect for third-order terms in this case tends to cancel that for second-order terms. The second- and third-order diagrams were calculated with the modifications just described to account for iterations of certain terms beyond third order. The result was  $\alpha_d = 5.569 \text{ \AA}^3$ .

In fourth order, new types of diagrams enter and examples are shown in Fig. 7. We may note that we have now included terms in which the correlations and DP interactions have assumed all possible relative positions. Diagrams 7(a), (b), and (f) may also be inverted and in 7(b) and (d) the first DP interaction may occur on the other particle line. When we have a single  $2p$  excitation, we multiply by the factor  $MF$  of Eq. (41). When the diagram begins or ends with a single excitation as for 7(a), (b), and (c), there is also the modification of the type shown in 7(f) which modifies 7(a). Numerical calculations of the diagrams of Fig. 7 are given in Table IX. Excited bound and continuum states were included for  $l=0, 1, \text{ and } 2$ .

The factor which results from the normalization  $\langle \Psi_0 | \Psi_0 \rangle$  in the denominator of Eq. (34) for  $\alpha_d$  must be

TABLE IX. Contributions to  $\alpha_d$  from diagrams of Fig. 7.\*

Diagram	Value in $\text{\AA}^3$
a	0.8484
b	0.4257
c	0.5957
d	0.3383
e	0.3389
f	-0.4232
Total	2.1238

\*  $1 \text{ \AA} = 10^{-8} \text{ cm}$ .

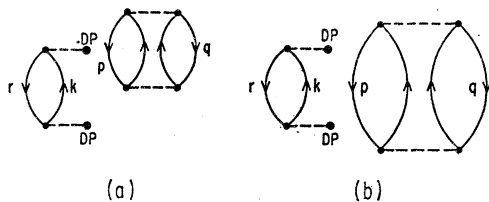


FIG. 8. Disconnected diagrams which factor when added. States  $p$  and  $q$  must be different from  $r$  and the excitations of  $p$  and  $q$  must differ from  $k$  because of the exclusion principle. Diagrams of this type give the factor of Eq. (45).

included. This effect of this factor is reduced when we consider the higher order terms of Fig. 8. When 8(a) and 8(b) are added, the disconnected parts factor into the product  $\alpha_d$  in second order ( $\alpha_d^{(2)}$ ) times the lowest order contribution of  $p, q$  to the correlation part of the normalization which is

$$Nm(p, q) = \sum_{kk'} |\langle pq | v | kk' \rangle|^2 / D^2, \quad (43)$$

$$\langle \Psi_0 | \Psi_0 \rangle = 1 + \sum_{pq} Nm(p, q). \quad (44)$$

Although the nondiagonal terms have not been explicitly written in Eq. (43), they are assumed included in  $Nm(p, q)$ . The diagrams like those of Fig. 8 and the normalization  $\langle \Psi_0 | \Psi_0 \rangle^{-1}$  combine to multiply  $\alpha_d^{(2)}(r \rightarrow k)$  by the factor

$$(1 + \sum_{pq \neq r} Nm'(p, q)) / (1 + \sum_{pq} Nm(p, q)). \quad (45)$$

The sums  $pq$  extend over all unexcited states except in the numerator where  $p$  and  $q$  must not equal  $r$  because of the exclusion principle. The prime in the numerator indicates that the excited state  $k$  is not to be included in calculating  $Nm(p, q)$ . The higher order diagrams for  $\alpha_d$  are treated similarly. Only connected terms are then retained, the corrections from disconnected terms being contained in Eq. (45). For a large system, Eq. (45) becomes effectively one. However, for a small system such as Be, the restrictions on the sum in the numerator of Eq. (45) may have an important effect. Calculations of the normalization terms  $Nm$  resulted in  $Nm(2s, 2s) = 0.1107$ ,  $Nm(1s, 1s) = 0.0028$ , and  $Nm(1s, 2s) = 0.000125$ . In calculating  $\langle \Psi_0 | \Psi_0 \rangle$ ,  $4Nm(1s, 2s)$  is included to account for the four  $1s-2s$  pairs. The total value for  $\alpha_d$  before normalization is  $7.69 \text{ \AA}^3$  and after normalization becomes  $6.93 \text{ \AA}^3$ . For Be the normalization effect is approximately 10%. This correction may be especially large for Be due to the low-lying  $2p$  excitation which enhances the effect of  $D^2$  in Eq. (43).

### B. The Dipole Shielding Factor

When an external charge  $Z'$  is placed at  $r'$ , the electric field at the nucleus due to the electrons divided by the

electric field at the nucleus due to  $Z'$  is defined as the dipole shielding factor  $\beta_\infty$ .

$$\begin{aligned} \beta_\infty &= \langle \langle \Psi | \sum_{i=1}^N P_1(\cos\theta_i) / r_i^2 | \Psi \rangle / \langle \Psi | \Psi \rangle \rangle (Z' / r'^2)^{-1} \\ &= 2 \langle \Psi_0 | \sum_{i=1}^N P_1(\cos\theta_i) / r_i^2 | \Psi_1^{(1)} \rangle / \langle \Psi_0 | \Psi_0 \rangle, \end{aligned} \quad (46)$$

where  $Z'$  is assumed small and terms of second and higher powers of  $Z'$  are neglected. The formula for  $\beta_\infty$  differs from Eq. (34) for  $\alpha_d$  only by the replacement of the second interaction  $U_1$  by the shielding term

$$S_1 = \sum_{i=1}^N P_1(\cos\theta_i) / r_i^2. \quad (47)$$

Therefore,  $\beta_\infty$  may be calculated analogously to  $\alpha_d$ , the second one-body interaction being  $S_1$ .

The formulas for  $\beta_\infty$  in second order are

$$\begin{aligned} \sum_{n=2}^{\infty} \beta_\infty(2s \rightarrow np) &= -4 \sum_{n=2}^{\infty} \langle 2s | r^{-2} \cos\theta | np \rangle \\ &\quad \times (\epsilon_{2s} - \epsilon_{np})^{-1} \langle np | r \cos\theta | 2s \rangle \end{aligned} \quad (48)$$

and

$$\begin{aligned} \sum_k \beta_\infty(2s \rightarrow kp) &= -(8/\pi) \int_0^\infty dk \langle 2s | r^{-2} \cos\theta | kp \rangle \\ &\quad \times (\epsilon_{2s} - k^2/2)^{-1} \langle kp | r \cos\theta | 2s \rangle. \end{aligned} \quad (49)$$

The  $1s$  contributions are obtained by replacing  $2s$  by  $1s$  in Eqs. (48) and (49). These equations are analogous to Eqs. (38) and (39) for  $\alpha_d$ . The second-order contributions to  $\beta_\infty$  given in Table X add to 4.296 which is in poor agreement with the theoretical value 1.00,<sup>19</sup> and so it is necessary to consider the higher order terms. There are terms of the same type as considered for  $\alpha_d$  and shown in Figs. 5, 6, and 7. In addition there are now important contributions from the  $1s$  electrons. This is not surprising as  $\beta_\infty$  involves matrix elements of  $r^{-2}$

TABLE X. Second-order contributions to the dipole shielding factor  $\beta_\infty$ .

$n$	$\beta_\infty(2s \rightarrow np)$	$n$	$\beta_\infty(1s \rightarrow np)$
2	3.88977	2	0.03267
3	-0.02783	3	0.00635
4	-0.01276	4	0.00240
5	-0.00612	5	0.00116
6	-0.00337	6	0.00065
7	-0.00205	7	0.00040
8	-0.00134	8	0.00026
$\sum_{n=9}^{\infty}$	-0.00422	$\sum_{n=9}^{\infty}$	0.000829
continuum	-0.01766	continuum	0.4373
2s total	3.814	1s total	0.482

<sup>19</sup> R. M. Sternheimer, Phys. Rev. 96, 951 (1954).

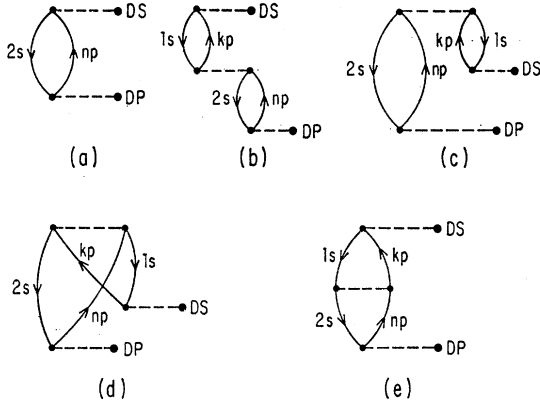


FIG. 9. (a) Second-order diagram for the dipole shielding factor  $\beta_{\infty}$ . (b), (c), (d), and (e) are third-order diagrams involving  $1s$  and  $2s$  states. In diagrams (d) and (e) the two hole states must have parallel spins.

which emphasizes the inner atomic regions. In the most important of these  $1s-2s$  terms shown in Fig. 9 the  $2s$  electron contributes to the  $r$  matrix element and the  $1s$  electron to  $r^{-2}$ . The line labeled DS represents the interaction with the shielding operator  $S_1$ . Diagram (c) may be inverted except that the DS interaction must appear above DP. Diagrams (b) and (c) are similar to  $2s-2s$  third-order diagrams except that one of the hole states is labeled  $1s$ . In diagrams (d) and (e) the hole states must have parallel spins.

When diagram 9(b) was calculated with the factor  $MF$  of Eq. (41) the result was  $-0.592$ . The sum of 9(c) and its inverted form was also  $-0.592$ . Diagram (d) was calculated to be  $-0.0489$  and (e) was  $-0.126$ . Additional modifications to these diagrams come from the fact that when there is a single  $1s$  excitation, the interactions with the potential do not exactly cancel interactions with the occupied unexcited states. This was found to give approximately a 10% increase to diagrams like (b) and (e). This increase was approximately canceled by inclusion of higher order  $1s-1s$  interactions which modify a single  $1s$  excitation in the same way that the single  $2s$  excitation in Fig. 5(a) is modified by 5(b) and (c).

The result of calculating the modified second- and third-order diagrams involving two  $2s$  electrons was found to be 1.248. The basic diagrams are shown in Figs. 5(a), (b), and (c) except that the topmost interaction is now DS rather than DP. The appropriate modifications to the basic diagrams were discussed in Sec. IV A. Similar calculations involving the two  $1s$  electrons gave the result 0.438. Calculation of the  $1s-2s$  diagrams of Figs. 9(b), (c), (d), and (e) gave the result  $-1.189$ . This number includes the modifications discussed above and a very small contribution from interactions of the basic diagrams. The modified total result through third order is then 0.498.

The final result was obtained by considering higher order diagrams of the type shown in Fig. 7 with DS

replacing the upper DP and by including the normalization factor of Eq. (45). The higher order diagrams included not only the basic structures of Fig. 7 but also the possible additions to them by adding on  $1s-2s$  interactions in the same way that diagrams in Figs. 9(b), (c), (d), and (e) may be considered as additions to the basic diagram of Fig. 9(a). Before normalization the higher order terms contributed 0.532, giving a total 1.030. After normalization the total dipole shielding result was 0.972. The normalization factors significantly affected (by approximately 10%) only the terms in which there was at least one  $2s$  electron excited.

### C. Quadrupole Polarizability

The quadrupole polarizability is defined by

$$\alpha_q \equiv 2 \langle \Psi_0 | \sum_{i=1}^N r_i^2 P_2(\cos\theta_i) | \Psi_1^{(2)} \rangle / \langle \Psi_0 | \Psi_0 \rangle. \quad (50)$$

The term  $\Psi_1^{(2)}$  is defined by Eq. (33) and is obtained from BG theory by collecting all the terms of  $\Psi$  given by Eq. (37) in which the perturbation  $-U_2$  acts once and only once. The calculation of  $\alpha_q$  proceeds in the same manner as that of  $\alpha_d$  except that the operator  $U_1$  is replaced by  $U_2$ .

The second-order formulas are

$$\sum_{n=2}^{\infty} \alpha_q(2s \rightarrow nd) = -4 \sum_{n=2}^{\infty} |\langle 2s | r^2 P_2(\cos\theta) | nd \rangle|^2 \times (\epsilon_{2s} - \epsilon_{nd})^{-1}, \quad (51)$$

$$\sum_k \alpha_q(2s \rightarrow kd) = -\frac{8}{\pi} \int_0^{\infty} dk |\langle 2s | r^2 P_2(\cos\theta) | kd \rangle|^2 \times (\epsilon_{2s} - k^2/2)^{-1}. \quad (52)$$

The angular integrations contribute a factor  $\frac{1}{5}$  on the right-hand side of Eqs. (51) and (52). Both equations contain a factor 2 for two  $2s$  electrons. The  $1s$  terms are obtained by substituting  $1s$  for  $2s$  in Eqs. (51) and (52).

The results of the second-order calculations are given in Table XI and the total second-order result is  $15.09 \text{ \AA}^5$ .

TABLE XI. Second-order contributions to the quadrupole polarizability.\*

$n$	$\alpha_q(2s \rightarrow nd) \text{ \AA}^5$	$n$	$\alpha_q(1s \rightarrow nd) \text{ \AA}^5$
3	6.7760	3	$6.889 \times 10^{-7}$
4	1.9161	4	$4.028 \times 10^{-7}$
5	0.8059	5	$2.326 \times 10^{-7}$
6	0.4184	6	$1.427 \times 10^{-7}$
7	0.2467	7	$9.293 \times 10^{-8}$
8	0.1583	8	$6.355 \times 10^{-8}$
9	0.1079	9	$4.525 \times 10^{-8}$
10	0.07701	10	$3.330 \times 10^{-8}$
$\sum_{n=11}^{\infty}$	0.3218	$\sum_{n=11}^{\infty}$	$1.444 \times 10^{-7}$
continuum	4.2620	continuum	0.000609
1s total	$15.0901 \text{ \AA}^5$	1s total	$0.000611 \text{ \AA}^5$

\*  $1 \text{ \AA}^5 = 10^{-40} \text{ cm}^5$ .

TABLE XII. Second-order contributions to the quadrupole shielding factor  $\gamma_\infty$ .

$n$	$\gamma_\infty(2s \rightarrow nd)$	$n$	$\gamma_\infty(1s \rightarrow nd)$
3	0.19430	3	$2.546 \times 10^{-5}$
4	0.07383	4	$1.514 \times 10^{-5}$
5	0.03537	5	$8.778 \times 10^{-6}$
6	0.01968	6	$5.385 \times 10^{-6}$
7	0.01208	7	$3.517 \times 10^{-6}$
8	0.00796	8	$2.405 \times 10^{-6}$
9	0.00552	9	$1.719 \times 10^{-6}$
10	0.00399	10	$1.252 \times 10^{-6}$
$\sum_{n=11}^{\infty}$	0.01928	$\sum_{n=11}^{\infty}$	$6.888 \times 10^{-6}$
continuum	0.51589	continuum	0.16987
2s total	0.88790	1s total	0.16994

The contribution from 1s terms is negligible. The third-order terms correspond to those in Figs. 5(b) and (c) for  $\alpha_d$  including the inverted form of 5(c). The interaction lines labeled DP now are labeled QP and correspond to the interaction  $U_2$ . The excited states are  $nd$  and  $kd$ . Since the correlations between two 2s electrons are given almost entirely by excitations into  $p$  states,<sup>5</sup> the third-order terms for  $\alpha_d$  were expected to be much less important than they were for  $\alpha_d$ . This was found to be true; the third-order terms contributed  $-1.034 \text{ \AA}^5$ , giving a total result  $14.06 \text{ \AA}^5$  for second- and third-order terms. Fourth-order terms were not calculated and the normalization factors were omitted for consistency as they correspond to fourth-order and higher terms. Most fourth-order terms are expected to increase the value for  $\alpha_d$ , and  $\alpha_d$  is reduced by the normalization factors so there should be some cancellation between these two effects. However, since  $l=1$  states may enter into the fourth-order terms, the fact that third-order terms are small does not necessarily imply fourth-order terms are also small.

#### D. The Quadrupole Shielding Factor

The quadrupole shielding factor  $\gamma_\infty$  is defined as the change in the gradient of electric field at the nucleus due to the electrons divided by the gradient of electric field at the nucleus due to the external charge  $Z'$ .

$$\gamma_\infty \equiv 2 \langle \Psi_0 | \sum_{i=1}^N r_i^{-3} P_2(\cos\theta_i) | \Psi_1^{(2)} \rangle / \langle \Psi_0 | \Psi_0 \rangle. \quad (53)$$

The second-order terms are

$$\sum_{n=2}^{\infty} \gamma_\infty(2s \rightarrow nd) = \sum_{n=2}^{\infty} -4 \langle 2s | r^{-3} P_2(\cos\theta) | nd \rangle (\epsilon_{2s} - \epsilon_{nd})^{-1} \times \langle nd | r^2 P_2(\cos\theta) | 2s \rangle, \quad (54)$$

$$\sum_k \gamma_\infty(2s \rightarrow kd) = -\frac{8}{\pi} \int_0^\pi dk \langle 2s | r^{-3} P_2(\cos\theta) | kd \rangle \times (\epsilon_{2s} - k^2/2)^{-1} \langle kd | r^2 P_2(\cos\theta) | 2s \rangle, \quad (54a)$$

and similarly for excitations of 1s electrons. The second order contributions to  $\gamma_\infty$  are given in Table XII. Both 1s and 2s contributions are now significant. More than half of the total result 1.058 comes from continuum states; this is not surprising since the wave function for  $nd$  states is generally far from the origin due to the centrifugal barrier and so the  $r^{-3}$  matrix elements are small. However, the continuum states have sufficient energy to overcome much of the barrier.

The third-order  $2s-2s$  terms which were calculated correspond to the third-order correction terms for  $\alpha_d$  shown in Fig. 5. However, the bottom interaction is now QP and the top interaction is through the quadrupole shielding (QS) term  $r^{-3} P_2(\cos\theta)$ . Excited states have  $l=2$ . Third-order terms involving  $1s-2s$  interactions of the types shown in Fig. 9 but with changes to QP, QS, and  $l=2$  excitations were also calculated. Corrections were made which account for the fact that for 1s excitations the interactions with the potential do not cancel interactions with occupied unexcited states. This effect gave a 7% increase to the terms with 1s excitations. The contributions from third-order  $2s-2s$  terms was calculated to be  $-0.144$  and from  $1s-2s$  terms  $-0.163$ . The  $1s-1s$  terms were small. The final result of these calculations is 0.751. The fourth-order and higher terms were not considered in calculating  $\gamma_\infty$  and it is possible that they might contribute significantly since excitations into  $l=1$  states are now possible. Very rough calculations of some fourth-order terms indicated that  $\gamma_\infty$  might increase by as much as 20% and  $\alpha_d$  change less. Any increase, of course, would be partly offset by the normalization factor. It is possible that the second-order result could turn out to be in better agreement with experiment than the result including third-order terms.

(Note added in proof. The results of this section are in good agreement with those of Professor A. Dalgarno who has used the coupled Hartree-Fock approximation for Be. An analysis of the coupled method indicates that it includes the second- and third-order diagrams of this section and higher iterations of these basic diagrams, and so the coupled method actually includes some of the correlation effects. I am grateful to Professor Dalgarno for forwarding his results prior to publication.)

#### VI. OSCILLATOR STRENGTHS

The oscillator strength  $f_{ni}^z$  for a transition between an initial state  $i$  and an excited state  $n$  is given in atomic units by<sup>20</sup>

$$f_{ni}^z = 2\omega_{ni} | \langle n | Z_{Op} | i \rangle |^2, \quad (55)$$

where  $Z_{Op} = \sum_{j=1}^N z_j$ . The energy difference between states  $n$  and  $i$  is given by  $\omega_{ni}$  in a.u. The ground state of Be is  $(1s)^2(2s)^2 1S$  and transitions are calculated to excited states  $(1s)^2(2s)(np) 1P$  which may be written in

<sup>20</sup> H. A. Bethe, *Intermediate Quantum Mechanics* (W. A. Benjamin, Inc., New York, 1964), Chap. 13, p. 147.

TABLE XIII. Excitation energies in a.u. from  $(2s)^2\ ^1S$  to  $(2s)(np)\ ^1P$ .

$n$	$\omega_{ni}^a$	$\omega_{ni}^b$
2	0.1935	0.1939
3	0.2467	0.2742
4	0.2749	0.3063
5	0.2877	
6	0.2946	
7	0.2986	
8	0.3012	
Ionization limit	0.3094	0.3426

<sup>a</sup> Calculated from Eq. (58).  
<sup>b</sup> Experimental values obtained from Ref. 21. Only values up to  $n=4$  were listed.

second quantized notation

$$|2sn\ \dot{p}\ ^1P\rangle = 2^{-1/2}(\eta_{2s^+}\eta_{np^-} - \eta_{2s^-}\eta_{np^+})|0\rangle, \quad (56)$$

when correlations in these states are neglected. The notation  $2s^+$ ,  $np^-$  indicates  $2s$  electron with spin up, etc. The state  $|0\rangle$  is the "core" state  $(1s)^2\ ^1S$ . The operators  $\eta^+$  satisfy the usual Fermi-Dirac anticommutation relations.<sup>2</sup> The excitation energy

$$\omega_{ni} = \langle 2sn\ \dot{p}\ ^1P | H | 2sn\ \dot{p}\ ^1P \rangle - \langle (2s)^2\ ^1S | H | (2s)^2\ ^1S \rangle. \quad (57)$$

If we use the ground-state Hartree-Fock solution for  $(2s)^2\ ^1S$  and Eq. (56) for  $(2s)(np)\ ^1P$  with the  $np$  single-particle orbitals determined by Eq. (13),

$$\omega_{ni} = \epsilon_{2p} - \epsilon_{2s} + \langle 2sn\ \dot{p} | v | np\ 2s \rangle. \quad (58)$$

The  $1s$  and  $2s$  orbitals used in  $(2s)(np)\ ^1P$  are the same as for  $(2s)^2\ ^1S$ .

Excitation energies calculated from Eq. (58) are given in Table XIII and are compared with the observed energies obtained from the Charlotte Moore

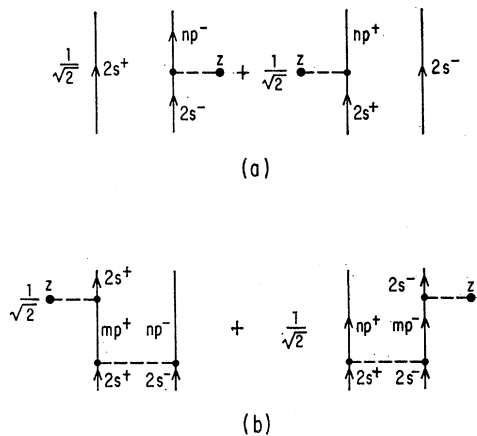


FIG. 10. Diagrams contributing to oscillator strength matrix elements. (a) Hartree-Fock approximation. (b) Correlation terms. These diagrams differ from the usual diagrams of Ref. 2 in that both hole and particle lines are directed upwards. The lines at the bottom of the diagrams represent single-particle states occupied in the initial state  $i$ . Lines at the top of the diagram represent single-particle states occupied in the final state  $n$ .

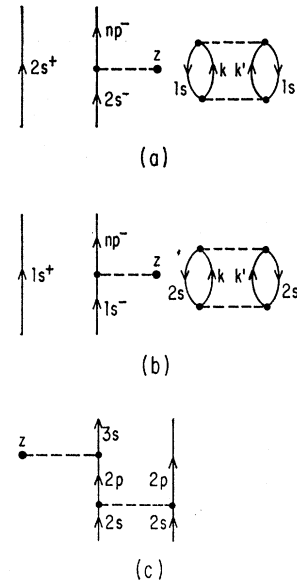


FIG. 11. Higher order diagrams contributing to oscillator strength matrix elements. (a) and (b) are disconnected diagrams. (c) Transitions  $(2s)^2\ ^1S \rightarrow (ns)\ \times (2p)\ ^1P$  are possible when correlations among the two  $2s$  electrons are included.

Tables.<sup>21</sup> The discrepancy between calculated and observed values increases with the excitations and is mostly due to omission of correlation corrections for the calculated energies. When a  $2s$  electron has been raised to a highly excited state it is expected to have little correlation energy with the remaining  $2s$  electron. If the  $2s-2s$  correlation energy of the ground state is included with the ionization limit calculated from Eq. (58), the result is 0.353 a.u. which improves agreement with the observed value 0.343 a.u.

When the oscillator strengths are calculated in the first approximation,

$$f_{ni} = 4\omega_{ni} |\langle np | z | 2s \rangle|^2. \quad (59)$$

This approximation for the matrix elements  $\langle n | Z_{Op} | i \rangle$  is illustrated by diagram (a) of Fig. 10. Unlike the usual many-body diagrams, both particle and hole lines point upwards; the lines at the bottom of the diagram correspond to the initial unexcited states of  $i$  and the lines at the top correspond to the unexcited single-particle states of the final state  $n$ . The ground-state Hartree-Fock determinant  $i$  is connected to each of the excited-state determinants in the linear combinations (56) through the matrix element  $\langle np | z | 2s \rangle$ . It is also desirable to include the effects of correlations among the two  $2s$  electrons in the ground state and these are represented by Fig. 10(b). The contribution to  $\langle n | G_{Op} | i \rangle$  from diagrams (a) and (b) together is

$$\langle n | Z_{Op} | i \rangle = \sqrt{2} (\langle np | z | 2s \rangle + \sum_m \langle 2s | z | mp \rangle D^{-1} \times \langle mpn\ \dot{p} | v | 2s\ 2s \rangle). \quad (60)$$

<sup>21</sup> Atomic Energy Levels, edited by C. E. Moore, Natl. Bur. Std. Circ. No. 467 (U. S. Government Printing Office, Washington, D. C., 1949), Vol. I.

TABLE XIV. Oscillator strengths for transitions  $(2s)^2 1S \rightarrow 2sn p^1 P$ .

$n$	$f_{ni}^z(\text{HF})^a$	$f_{ni}^z(\text{corr})^b$
2	2.0293	1.2540
3	0.00541	0.01676
4	0.00530	0.01013
5	0.00318	0.00549
6	0.00194	0.00321
7	0.00125	0.00202
8	0.00084	0.00135
$\infty$		
$\sum_{n=9}$	0.00295	0.00467

<sup>a</sup> Calculated from Eq. (59) using Hartree-Fock single-particle states.

<sup>b</sup> Ground-state correlations are included in these values.

The denominator  $D$  is calculated by Eq. (18) to account for higher order terms and account is also taken of non-diagonal terms as explained in Sec. IV. There is still the normalization correction to be considered because the correlated ground state is obtained by BG theory and in Eq. (55) it is assumed that states  $n$  and  $i$  are normalized to unity. Most of the normalization corrections come from  $2s$  electrons and the very small effects from  $1s$  contributions to the normalization are essentially canceled by terms of the form shown in Fig. 11(a). A more detailed analysis of this point is given later in this section. Oscillator strengths calculated by Eq. (59), using single-particle Hartree-Fock states of Eq. (13), are compared in Table XIV with those calculated with correlation and normalization corrections. The observed excitation energies listed in Table XIII were used and extrapolations were made to obtain higher excitation energies. The values in Table XIV may be compared with the results of Altick and Glassgold<sup>22</sup> who used Hartree wave functions and employed the methods of the random-phase approximation.<sup>23</sup> Their oscillator strength for the  $n=2$  transition is 2.34 using Hartree single-particle states and 1.71 including correlations by the random-phase approximation. For the higher levels, their Hartree oscillator strengths are larger than the Hartree-Fock values listed here but their correlated values are lower than the Hartree-Fock values of the present calculation.

It is of interest also to compute the oscillator strengths of  $1s$  excitations to bound excited states and those for  $1s$  and  $2s$  transitions to the continuum so that we may evaluate the Thomas-Reiche-Kuhn sum rule.<sup>20</sup>

$$\sum_n f_{ni}^z = N. \quad (61)$$

When  $1s \rightarrow np$  or  $1s \rightarrow kp$  transitions are calculated, terms of the form shown in Fig. 11(b) should be included. These account for correlations among the two unexcited  $2s$  electrons. These correlations should also be included in the normalization for both the ground state  $i$  and excited state  $n$ . Because the particles in

excited states are propagating in the presence of different unexcited states above and below the  $z$  interaction, the denominators as given by Eq. (18) are different in these two cases. The correlation part of Fig. 11(b) is

$$|\langle 2s2s | v | kk' \rangle|^2 / D_n D_i, \quad (62)$$

where  $D_i$  is the denominator for  $(1s)^2$  occupied and  $D_n$  is the appropriate denominator when  $1s^+$  and  $np^-$  are occupied. For  $1s$  transitions, Eq. (55) then becomes

$$f_{ni}^z = 2\omega_{ni} |\langle n | Z_{0p} | i \rangle|^2 (1 + \sum'_{kk'} |\langle 2s2s | v | kk' \rangle|^2 / D_n D_i)^2 \\ \times [(1 + \sum_{kk'} |\langle 2s2s | v | kk' \rangle|^2 / D_n^2) \\ \times (1 + \sum'_{kk'} |\langle 2s2s | v | kk' \rangle|^2 / D_i^2)]^{-1}. \quad (63)$$

The prime in the first sum indicates  $k, k'$  do not equal the excited single-particle state in  $n$ . The subscript  $c$  after  $|\langle n | Z_{0p} | i \rangle|^2$  indicates that only connected terms are included. This means that terms as shown in Fig. 11(b) are not to be included as they are accounted for by the factor following  $|\langle n | Z_{0p} | i \rangle|^2$ . All normalization corrections are accounted for by the last factor of Eq. (63). The sums over  $k$  and  $k'$  include all excited states although for Be the  $(2p)(2p)$  excitation dominates. The terms  $|\langle 2s2s | v | kk' \rangle|^2$  should include appropriate factors to account for the small nondiagonal correlation terms discussed in Sec. V. For example, we may multiply  $\langle kk' | v | 2s2s \rangle$  by the factor

$$1 + \left( \sum_{k''k''' \neq kk'} \langle kk' | v | k''k''' \rangle D^{-1} \langle k''k''' | v | 2s2s \rangle \right) \\ \times \langle kk' | v | 2s2s \rangle^{-1}, \quad (64)$$

which accounts for nondiagonal particle-particle interactions, and similarly for particle-hole interactions.  $D_i$  is given by Eq. (18) with  $p, q$  replaced by  $2s, 2s$  and  $D_n$  becomes

$$D_n = (\epsilon_{2s} - \langle 2s1s | v | 2s1s \rangle + \langle 2sn p | v | 2sn p \rangle) \\ + (\epsilon_{2s} - \langle 2s1s | v | 2s1s \rangle + \langle 2s1s | v | 1s2s \rangle) \\ + \langle 2sn p | v | 2sn p \rangle - \langle 2sn p | v | np2s \rangle \\ - (\epsilon_k - \langle k1s | v | k1s \rangle + \langle kn p | v | kn p \rangle) \\ - (\epsilon_{k'} - \langle k'1s | v | k'1s \rangle + \langle k'1s | v | 1sk' \rangle) \\ + \langle k'n p | v | k'n p \rangle - \langle k'n p | v | npk' \rangle - \langle 2s2s | v | 2s2s \rangle \\ - \langle kk' | v | kk' \rangle + \langle k2s | v | k2s \rangle + \langle k'2s | v | k'2s \rangle \\ + E_{\text{corr}}(2s, 2s; 1sn p \text{ unex}) + 2E_{\text{corr}}(2s, 1s; 1sn p \text{ unex}) \\ + 2E_{\text{corr}}(2s, np; 1sn p \text{ unex}). \quad (65)$$

The correlation terms in Eq. (65) are written so as to emphasize the fact that the correlations are computed for the state  $(1s)(np)(2s)^2$ . The terms added to the single-particle energies  $\epsilon$  account for the fact that the single-particle states were computed in the potential field of the nucleus and  $(1s)^2(2s)$  but one  $1s$  electron is now in the state  $np$ .

<sup>22</sup> P. L. Altick and A. E. Glassgold, Phys. Rev. 133, A632 (1964).

<sup>23</sup> K. Sawada, Phys. Rev. 106, 372 (1957).

TABLE XV. Sum-rule evaluation for oscillator strengths in Be.

Transitions	Hartree-Fock	Correlated
$2s \rightarrow np$	2.0499	1.2977
$2s \rightarrow kp$	0.6420	0.5969
$1s \rightarrow np$	0.2091	0.2029
$1s \rightarrow kp$	2.0663	1.9744
$(2s)^2 \rightarrow (ns)(2p)$		0.0690
Total	4.967	4.141

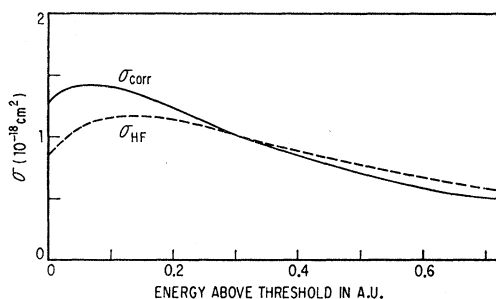
When the state  $np$  is in the continuum the matrix elements of Eq. (65) which involve this state are zero because of the continuum states' normalization  $(2/R_0)^{1/2}$ , where  $R_0$  is the radius of a large sphere tending to infinity.<sup>5</sup> For  $np$  in the continuum,  $D_n=0.438$  for  $k$ ,  $k'=2p$ ,  $2p$  and  $m_i=\pm 1$  from Eq. (65). For comparison,  $D_i=0.3212$  for two  $2p$  excitations and  $m_i=\pm 1$ . Calculation of the factors on the right of Eq. (63) which multiply  $|\langle n|Z_{0p}|i\rangle|^2$  gave the result 0.993 for  $np$  in the continuum.

The sum rule of Eq. (61) was evaluated and the results are given in Table XV. The transitions  $(2s)^2\ ^1S \rightarrow (ns)(2p)\ ^1P$  are possible only when correlations of the two  $2s$  electrons are included. The process is shown in Fig. 11(c). The most important transition is  $(2s)^2 \rightarrow (3s)(2p)\ ^1P$  for which the oscillator strength was found to be 0.0642. The correlated sum rule result 4.14 is in considerably better agreement with the theoretical value 4.00 than is the Hartree-Fock result 4.97.<sup>24</sup>

The Be photoionization cross section  $\sigma_k$  for transitions of a  $2s$  electron into a continuum  $p$  state is

$$\sigma_k = 4\pi^2 \frac{\omega_B \alpha}{k} \sum_{M_L=-L}^{+L} |\langle 2snp\ ^1P(M_L) | Z_{0p} | (2s)^2\ ^1S \rangle|^2, \quad (66)$$

where the continuum electron has energy  $k^2/2$ ,  $\omega_B$  is the ionization potential plus  $k^2/2$ , and  $\alpha$  is the fine structure constant.<sup>25</sup> The continuum function in this case has the normalization factor  $(2/\pi)^{1/2}$ . The cross section  $\sigma_k$  is plotted in Fig. 12. The curve labeled "corr" includes correlation effects from the two  $2s$  electrons in


 FIG. 12. Photoionization cross sections for Be( $2s \rightarrow kp$ ).

<sup>24</sup> The term "Hartree-Fock result" means that correlations are not included and the calculations used the single-particle states of Eq. (13), except for  $\varphi_{1s}$ , obtained from Ref. 8.

<sup>25</sup> M. J. Seaton, Proc. Roy. Soc. (London) A208, 408 (1951).

the ground state and also the normalization factor. The excited state  $(2s)(kp)\ ^1P$  is obtained from the Hartree-Fock single-particle states of Eq. (13) and does not include correlations. The curve labeled  $\sigma_{\text{HF}}$  omits the correlation and normalization corrections of the ground state.

## VII. DISCUSSION AND CONCLUSIONS

In the previous sections it was shown that many-body perturbation theory may be used to obtain many varied atomic properties from correlation energies to oscillator strengths. Much of the value of this approach lies in the fact that once the set of single-particle states for the perturbation theory has been calculated and used for one property, it is relatively easy to use the same states and many of the matrix elements from the first calculation to obtain additional atomic properties. Also, from the evaluation of diagrams for one calculation, one often develops a physical feeling as to which diagrams will be important in other calculations since many of the matrix elements and denominators are equal in different diagrams. In many cases it is possible to relate quantitatively the diagrams for different calculations.

The convergence of the perturbation expansion is strongly dependent on the choice of the basis set of single-particle states, and in Sec. II it was pointed out that it is desirable to choose the potential in such a way that the excited states correspond essentially to the physical single-particle excitations. This approach, which is a departure from the previous use of the Hartree-Fock potential in Ref. 5, was justified in Sec. II. For all atoms there is now an infinite number of excited bound states and the continuum to be included in the perturbation expansion. However, it was shown in the calculations of Secs. III, IV, V, and VI that perturbation calculations are readily made using this set of states and the convergence of the expansion is much more rapid than in Ref. 5. The sums over the infinite number of bound excited states were easily carried out by use of the  $n^{-3}$  rule which was demonstrated in Sec. III.

The correlation energy for Be  $2s$  electrons excited into  $l=1$  states was found to be  $-0.0436$  a.u. as compared with  $-0.0426$  a.u. calculated in K. This particular calculation was repeated in this paper since in K the perturbation expansion converged very slowly for  $2s$  correlations and the accuracy of the calculation was estimated to be approximately 5%. However, with the basis set of this paper the convergence was quite rapid and the accuracy of the result is estimated at better than 1%.

The perturbation theory may also be used to calculate other quantities such as polarizabilities and shielding factors as shown in Sec. V. The perturbation is more complicated than in the correlation energy calculation because there is now an additional perturbation due to the presence of an external charge. The second-order

result for the dipole polarizability  $\alpha_d$  was found to be  $12.15 \text{ \AA}^3$  but when the higher order terms were included the result was changed to  $6.93 \text{ \AA}^3$  with an expected accuracy of a few percent. The higher order terms are particularly important in this case because the two  $2s$  electrons have strong correlations into  $l=1$  states. This result may be compared with the second-order calculations of Kelly and Taylor<sup>17</sup> which gave  $4.54 \text{ \AA}^3$ . As pointed out by KT,<sup>17</sup> their approach is equivalent to the uncoupled Hartree-Fock approximation of Dalgarno<sup>15</sup> which also yielded  $4.5 \text{ \AA}^3$ . The second-order result of KT differs greatly from the second-order result of this paper because of the different basis sets of single-particle states. There are propagation corrections to the second-order calculations of KT because the interactions of excited states with the occupied unexcited states do not cancel the interaction with the Hartree-Fock potential. Since there is partial cancellation between the propagation corrections shown in Fig. 5(d) and the correlation terms of Figs. 5(b) and (c), the approach of KT can give reasonable results in second order when the correlations are strong. In this case the second-order results of this paper are poor and higher order terms must be included. However, when the correlations become small the propagation corrections do not necessarily also become small; and the second-order calculations of KT and of Dalgarno's uncoupled Hartree-Fock method may give results which are less than the correct solution. In general, it should be preferable to use either the coupled Hartree-Fock method of Dalgarno<sup>15</sup> or the perturbation theory approach presented in this paper for calculating polarizabilities and shielding factors. Dalgarno has previously pointed out that the coupled Hartree-Fock method is much more accurate than the uncoupled method.<sup>15</sup>

The dipole shielding calculations gave the second-order result 4.296 which is considerably higher than the 1.77 result of KT. This second-order difference has the same explanation as for  $\alpha_d$ . After the higher order terms were included, the final result was 0.972, with an estimated accuracy of approximately 5%. This value is in good agreement with the theoretical value 1.00. In order to obtain the value 0.972, it was necessary to consider all types of diagrams and the calculations were more complicated than for  $\alpha_d$  because of large effects from diagrams involving  $1s-2s$  correlations. The calculation of higher order diagrams may also be carried out with the basis set used by KT as shown in K. However, it is then necessary to sum diagrams like that of Fig.

5(d). The basis set of this paper sums these diagrams exactly and seems to be both more accurate and more convenient when higher order terms are to be included.

The calculated quadrupole polarizability was  $15.09 \text{ \AA}^5$  in second order and was changed to  $14.06 \text{ \AA}^5$  by inclusion of third-order terms. Again the second-order result is much higher than  $9.26 \text{ \AA}^5$  as calculated by KT. The accuracy of the second- and third-order calculations is expected to be within 2%. However, there is no assurance that the fourth-order terms which have been omitted are small. The calculated quadrupole shielding factor  $\gamma_\infty$  was 1.06 in second order as compared with 0.67 computed by KT. After inclusion of third-order terms  $\gamma_\infty$  was reduced to 0.75. The  $1s-2s$  correlations contributed significantly to the third-order terms for  $\gamma_\infty$  just as for  $\beta_\infty$ .

The methods of Sec. V may be readily applied to the calculation of higher order polarizabilities and shielding factors and it is probably a good approximation to limit these calculations to second order because correlations in higher  $l$  states are expected to be quite small.

In Sec. VI it was shown that the basis set of single-particle states of this paper is also useful in calculating quantities such as excitation energies, oscillator strengths, and photoionization cross sections. Correlations generally were included only for the ground state where they are expected to be most important. However, in a more detailed calculation the correlations in the excited states could also be included. The accuracy of these calculations is indicated by the evaluation of the sum rule which is theoretically 4.00 and was calculated as 4.14 including ground-state correlations and 4.97 without correlations.

The numerical calculations of this paper were for Be which has only four electrons and a simple closed shell structure. However, the perturbation theory is applicable to other atoms and may be particularly useful for atoms with a large number of electrons. In addition, many of the features of the perturbation theory which were used in the previous sections may be applied not only to other atoms but to other types of finite systems.

#### ACKNOWLEDGMENTS

I would like to thank Professor Keith A. Brueckner for his support and for very helpful suggestions, Dr. Howard S. Taylor for stimulating my interest in polarizability and shielding calculations, and Dr. Robert H. Traxler for helpful discussions.